THE ROLE OF CD49f - INTEGRIN α6- IN HUMAN STEM CELL BIOLOGY

by

SURAJ TIMILSINA

A Dissertation submitted in partial fulfillment of the
requirements for the degree of

DOCTOR OF PHILOSOPHY IN BIOLOGICAL AND BIOMEDICAL SCIENCES

2021

Oakland University
Rochester, Michigan

Doctoral Advisory Committee:

Luis Villa-Diaz, Ph.D., Chair
Shailesh K. Lal, Ph.D.
Gerard Madlambayan, Ph.D.

To my parents, Ram Kumari and Bal Krishna Timilsina, and to the love of my life, Kuttushree.

ACKNOWLEDGMENTS

I would like to sincerely thank my mentor, Dr. Luis Villa-Diaz, for his continuous encouragement, guidance, and support in my academic endeavors. In my time in his laboratory, I have grown so much as a person and as a scientist. Having spent five complete years in his lab as a graduate student has been a blessing to me. He has been the mentor that I have needed at every step of the way, always encouraging me to never stagnate in my pursuit of knowledge and to remain strong even during the toughest trials in life.

I would also like to thank my committee members, Dr. Shailesh K. Lal and Dr. Gerard Madlambayan for their time spent reading this manuscript and for their guidance during my dissertation proposal and annual reviews.

I would also like to thank my family for their kindness, love, support, and for always pushing me when I needed it. They have all been a source of inspiration, good humor, and perpetual motivation throughout my academic studies.

My sincerest gratitude is extended to all of my fellow graduate students and kind and very co-operative staffs in the Department of Biological Sciences. I am sincerely thankful to all of you for continuously offering me wisdom, friendship, and inspiration for me to become the highest quality and most genuine type of scientist and person that I am capable of.

Thank you all from the bottom of my heart. I couldn't have done this without you.

Suraj Timilsina

ABSTRACT

THE ROLE OF CD49f - INTEGRIN α6- IN HUMAN STEM CELL BIOLOGY

by

SURAJ TIMILSINA

Adviser: Luis Villa-Diaz, Ph.D.

Owing to the intrinsic capability for unlimited self-renewal and the ability to make all the cells in the body, pluripotent stem cells (PSC) are an ideal candidate to be used as starting material for cell therapies. The development of a standard human PSC (hPSC), which includes embryonic stem cells (hESC) and induced pluripotent stem cells (hiPSC), culture methods using completely defined and xeno-free culture environment will advance our knowledge of hPSC biology, and also increase the effectiveness of hPSC expansion on defined conditions for potential human applications.

It has been shown that stem cell fates are controlled by their specialized microenvironment, the stem cell niche, via direct cell-cell interactions, cell-extracellular matrix (ECM) contact- largely by surface proteins known as integrins- and the molecular signals emitting from the niche. Activation of integrins by binding to their ligands triggers signal transduction mechanisms involved in cell fate determination. In addition, because of their cell surface localization, integrins are used as biological markers to identify cell populations, and in this regard, integrin α6 (ITGA6), also known as CD49f, is a key biomarker identifying stem cells as it is commonly expressed in all identified stem cell types. Although, numerous findings strongly suggest that CD49f plays

important functions in stem cell biology, the underlying molecular mechanisms by which CD49f sustain stem cell's self-renewal have been only partially described.

In this project I have established a chemically defined and xeno-free culture condition for long-term maintenance and derivation of hPSC using chemically defined and xeno-free culture conditions. I also described a novel molecular mechanism involved in the maintenance of self-renewal and proliferation of hPSC using simulated microgravity (sμg). Moreover, my results highlighted CD49f as a reliable biomarker in identifying and characterizing functional status of human mesenchymal stem cells (hMSC).

TABLE OF CONTENTS

TABLE OF CONTENTS---Continued

TABLE OF CONTENTS---Continued

TABLE OF CONTENTS---Continued

LIST OF TABLES

LIST OF FIGURES

LIST OF FIGURES---Continued

LIST OF ABBREVIATIONS

bFGF	Basic fibroblast growth factor
BMP4	Bone morphogenetic proteins
BSA	Bovine serum albumin
CDK	Cyclin-dependent kinase
CD49f	Cluster of differentiation 49f
CDKI	Cyclin-dependent kinase inhibitors
CDM	Chemically defined medium
D-PBS	Dulbecco's phosphate buffered saline
DMEM	Dulbecco's modiefied eagles meedium
EB	Embryoid bodies
ECM	Extracellular matrix
EGF	epidermal growth factor
ESCs	Embryonic stem cells
E2f	E2F transcription factor
FACS	Fluorescence-activated cell sorting
FAK	Focal adhesion kinase
FBS	Fetal bovine serum
FGF4	Fibroblast growth factor 4
GATA4	GATA-binding protein 4
hESC	Human embryonic stem cells
hFF	Human foreskin fibroblasts

hiPSC	Human induced pluripotent stem cells
HS	Human serum
HSt	Human serum pre-conditioning
ICM	Inner cell mass
ILK	Integrin linked kinases
iPSC	Induced pluripotent stem cell
ITGA6	Integrin alpha6
ITGB1	Integrin beta1
ITGB4	Integrin beta4
KLF4	Kruppel-like factor 4
mESC	Mouse embryonic stem cells
MIDAS	Mg^{2+} ion in the metal-ion-dependent adhesion site
MSC	Mesenchymal stem cells
NANOG	NANOG homeobox
OCT4	Octamer-binding transcription factor-4
PBS	Phosphate buffered saline
PCR	Polymerase chain reaction
PMEDSAH	poly[2-(methacryloyloxy) ethyl dimethyl-(3-sulfopropyl) ammonium hydroxide]
PMEDSAH-g	poly[2-(methacryloyloxy) ethyl dimethyl-(3-sulfopropyl) ammonium hydroxide]- grafted
PSI	Plexin-sempahorin-integrin

p16	INK4a p16 kinase inhibitor 4a
p21	Cip1 p21 cyclin-dependent kinase inhibitor 1
p27	Cyclin-dependent kinase inhibitor 1B (CDKn1b)
p53	Tumor protein p53
pRb	Retinoblastoma protein
RA	Retinoic acid
SOX2	Sex determining region Y-box 2
SSEA-4	Stage-specifi c embryonic antigen 4
SSC	Skeletal stem cells
SUG	Simulated microgravity
TE	Trophectoderm
TERT	Telomerase reverse transcriptase
TGF-β1	Transforming growth factor beta 1
UG	Microgravity
XF	Xeno-free

CHAPTER ONE

BACKGROUND AND SIGNIFICANCE

1.1: Human Stem Cells as Experimental Model

1.1.1: Statement of the Problem

Three basic categories of cells make-up the human body: germ cells, somatic cells and stem cells. A stem cell has the ability to divide indefinitely and to give rise to mature specialized cell types. In other words, when a stem cell divides, the daughter cells can either enter a path leading to the formation of a differentiated specialized cell or self-renew to remain a stem cell, thereby ensuring that a pool of stem cells is constantly replenished in adult organs (1).

It has been shown that stem cell fates are controlled by their specialized microenvironment, the stem cell niche, via direct cell-cell interactions, cell-extracellular matrix (ECM) contact and the molecular signals emitting from the niche. Stem cells are anchorage-dependent cells and are bound to ECM largely by cell surface proteins known as integrins. Integrins are a large family of receptors which play key roles in cellular adhesion to ECM ligands and adjacent cells and serve as a link between extracellular components (matrisome), the cytoskeleton and non-receptor serine/threonine and tyrosine kinases. In mammals, there are 24 known heterodimeric integrin receptors comprising of a non-covalent pairing of one of 8 β subunits with one of 18 α subunits; and each with unique substrate affinities to ECM components including laminins, collagens, and fibronectin, as well as specific and non-redundant functions (2, 3).

Activation of integrins by binding to their ligands triggers signal transduction mechanisms involved in survival, shape, proliferation, motility, polarity, gene expression, cell differentiation, and apoptosis (4). In addition, because of their cell surface localization, integrins are used as biological markers to identify cell populations, and in this regard, integrin α6 (CD49F), also known as CD49f, is a key biomarker identifying stem cells (5). CD49f is identified as the only biomarker commonly expressed in all 35 identified populations of stem cells, including pluripotent stem cells (PSC) (which includes embryonic stem cells (ESC) and induced Pluripotent stem cells (iPSC)), somatic stem cells and cancer stem cells (5). CD49f distinguish stem cells from progenitor cells and differentiated somatic cells of their lineages (6). In the cardiac lineage, for example, CD49F is highly expressed in cardiac stem cells and atrial cardiomyocytes, while its expression is lower in ventricular cardiomyocytes, and absent in cardiac fibroblasts (7).

CD49F forms heterodimers with integrin B1 (ITGB1, also known as CD29) and/or integrin B4 (ITGB4, also known as CD104), to function as laminin receptors (2). ITGB4 is reported to be found in one stem cell population (8, 9), while ITGB1 (10-20) and laminins (21-28) have been identified in 11 stem cell populations. Furthermore, it has been shown that both ITGB1 and laminin contribute to regulating the balance between self-renewal and differentiation in several stem cell populations (29). While these findings strongly suggest that CD49f plays important functions in stem cell biology, the underlying molecular mechanisms by which CD49f sustain stem cell's self-renewal have been only partially described. Thus, further elucidation of these mechanisms is critical to advance our understanding of stem cell regulation. In the present work I will explore the

role of α6 integrin in regulating the fate of human stem cells (self-renewal and differentiation).

1.1.2: Stem Cells and Their Biological Properties and Classification

Stem cells are a subset of unspecialized cells that are found in multicellular organisms. They have the unique abilities to replenish themselves through self-renewal and to differentiate into different types of mature cells, which play essential roles in organogenesis during embryonic development and tissue regeneration (30, 31). Since the 1980's when stem cells were first isolated, scientists have been working to understand their behavior and properties in hopes of altering care of individuals with hematologic, oncologic, dermatologic, ophthalmologic, and orthopedic conditions. In recent years, there has been a great increase in our understanding of stem cell biology. The potential clinical applications lead to an extended interest in the use of stem cells in many medical disciplines. The most important role stem cells play in medicine is in cell therapy – replacement of cells that have been lost, destroyed, or altered.

Most of the 300 trillion cells of the body have completely specialized functions. Blood, lung, brain, skin or liver cells are all specialized for what they do. Stem cells, on the other hand, do not have a specialized function; they are an immature/unspecialized kind of cells that still have the potential to develop into many different cell types (32). Blastocysts, formed 4 to 5 days after the ovum is fertilization, are composed of two distinct cell types: the trophectoderm (TE, which will give rise to placental tissue) and the inner cell mass (ICM), which develops into epiblasts and induces the development of a fetus and also if isolated in the right in vitro conditions form embryonic stem cells (ESC) (33). Blastocysts are responsible for the regulation of the ICM microenvironment. As the

TE continues to develop and begins to form specialized support structures needed for the successful uterus implantation of the embryo, such as the placenta, the ICM cells remain pluripotent and proliferative. The pluripotency of stem cells allows them to form any cell of the organism (34). During the process of embryogenesis, cells form aggregations called germ layers: endoderm, mesoderm and ectoderm (Fig. 1.1.3(35)), each eventually giving rise to differentiated cells and tissues of the fetus and, later on, the adult organism. After ESC differentiate into one of the germ layers, they become multipotent stem cells, whose potency is limited to only the cells of that particular germ layer. After that, multipotent stem cells exist all over the organism as undifferentiated cells, and their key abilities are proliferation by the formation of the next generation of stem cells and differentiation into specialized cells under certain physiological conditions.

Signals that influence the stem cell specialization process can be divided into external, such as physical contact between cells or chemical secretion by surrounding tissue, and internal, which are signals controlled by the expression and transcription of genes.

The ESC can be described as pluripotent because they are able to eventually differentiate into every cell type in the organism as their in vivo counterpart, the ICM. Somatic or adult stem cells, on the other hand, are found in specialized niches among differentiated cells in the body during development and adult life. The function of these cells is to enable the healing, growth, and replacement of cells that are lost each day, by reaching end of their live cycle, by damage and/or diseases.

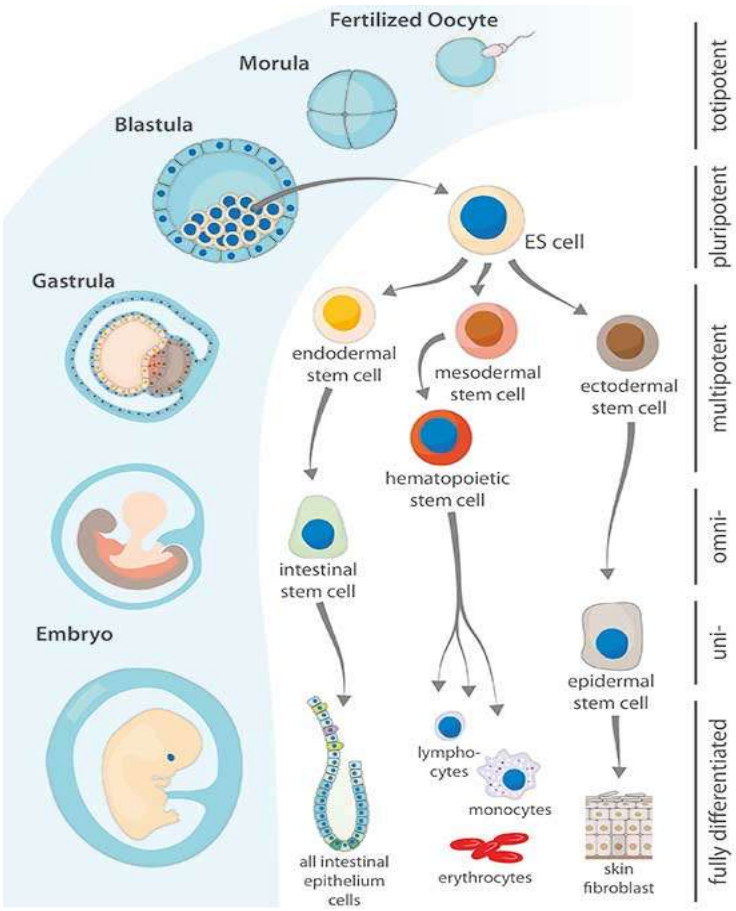

Figure 1.1.3: The potency tree of stem cells. The more developed stem cells become, and the more committed to their lineage, the lower their potential to give rise to different types of cells. A few exemplary stem cell lineages and some of their progeny are depicted.

In addition to being unspecialized, all stem cells have two additional properties: self-renewal, and potency. They can reproduce over and over again through asymmetric cell division, the newly produced offspring cells preserve the characteristics of the mother cell that has a different potency and lineage potential, such as a committed progenitor that

transiently amplifies to make several offspring. Most progenitor cells are multipotent or unipotent; therefore, they are also compared to adult stem cells. But they are in 'center' between stem cells and fully differentiated cells. Progenitor cells are usually found in adult organisms where they act as a repair system for the body. They replenish special cells and also maintain blood, skin, and intestinal tissues (1, 34). Examples of progenitor cells include satellite cells in muscles, bone marrow stromal cells, etc.

Below is a glossary of words that are frequently used in these project

Self-renewal: The ability of cells to proliferate without the loss of differentiation potential and without undergoing senescence (biologic aging). Stem cells are hypothesized to be able to divide symmetrically (in which both daughter cells are either stem cells or differentiated cells) or asymmetrically (yielding one stem cell and one more differentiated cell).

Homing: A process by which stem cells reach and stablish into the different parts of the body.

Plasticity: The ability of stem cells to differentiate into cell types beyond the tissues in which they normally reside.

Potency: Stem cells exist both in embryos and adult cells. There are several steps of specialization. Developmental potency is reduced with each step, which means that a unipotent stem cell is not able to differentiate into as many types of cells as a multipotent or a pluripotent one. Hence, potency is the ability to differentiate into different cell types, and can be either totipotent, pluripotent, multipotent, or unipotent.

- Totipotent cells have the capability to produce all cell types of the developing organism, including both embryonic and extraembryonic (such as placenta)

tissues. Example is a zygote. These cells can later develop either into any of the three germ layers or form a placenta. After approximately 4 days of the zygote formation, the blastocyst's inner cell mass becomes pluripotent and is the source of pluripotent cells.

- Pluripotent stem cells (PSC) form cells of all germ layers but not extraembryonic structures. Embryonic stem cells (ESC) are an example. Another example is induced pluripotent stem cells (iPSC). Their pluripotency is a continuum, starting from completely pluripotent cells and ending on representatives with less potency - multi-, oligo- or uni-potent cells.
- Multipotent stem cells have a narrower spectrum of differentiation, but they can specialize in discrete cells of specific cell lineages. One example is a hematopoietic stem cell, which can develop into several types of blood cells. After differentiation, a hematopoietic stem cell becomes an oligo-potent cell whose differentiation abilities are then restricted to cells of its lineage. In day 10 to 14 post-fertilization in the human, most stem cells are restricted to be either multipotent or unipotent.
- Unipotent cells make cells of a single cell type. An example is a germ cell, a stem cell that only makes the cells that mature to become egg or sperm.

1.1.3: Sources of Stem Cells

Embryonic Stem Cells

Embryonic stem cells are derived from the embryo. In humans, they are derived 7-10 days after fertilization from the pre-implantation blastocyst. As mentioned above, ES cells are pluripotent (36).

Adult stem cells

Adult stem cells, also known as somatic stem cells, are undifferentiated pluripotent or multipotent cells, found throughout the body after embryonic development that multiply by cell division to replenish dying cells and regenerate damaged tissues. They persist throughout life, and have been identified in many tissues including brain, bone marrow, blood vessels, heart, liver, and others. However, unlike embryonic stem cells, which are defined by their origin (the inner cell mass of the blastocyst), the origin of adult stem cells in some mature tissues is still under investigation (37).

Induced pluripotent stem cells

In 2006, an experiment was done in which genes that were usually expressed in ESC were introduces into mature cells. This process called genetic reprogramming, lead a small number of mature cells to revert back to a highly immature cell state that resembled an ESC. It induced a pluripotent state in a previously differentiated cell, hence the name (38).

1.1.4: Major Historical Perspective in Stem Cell Research

The discovery of stem cell populations has been an ongoing effort of several decades. The term ‘stem cell’ goes far as back as 1908 when the Russian histologist Alexander Maximow developed and introduced a theory of hematopoiesis, a theory upon which our present concept of blood cells' origin and differentiation is based(39).
The presence of self-renewing cells in mouse bone marrow was first illustrated in 1963 by McCulloch *et al* (40). In 1968, the first successful bone marrow transplant between two siblings was done. Hematopoietic stem cells were discovered in human cord blood in the year 1978. Martin *et al* (41)derived ESC from the inner cell mass of mouse embryos

in 1981. Gail Martin is attributed for coining the term "embryonic stem cell." The first evidence of cancer stem cell was observed in 1997. Leukemia is shown to originate from a hematopoietic stem cell. A year later, James Thomson and co-workers at University of Wisconsin-Madison derived the first human ESC line (42, 43).

In 2006, Professor Shinya Yamanaka and his group published the groundbreaking work about induced pluripotency in stem cell research. By the end of 2007, a Nobel Prize was awarded to Mario Capecchi, Martin Evans, and Oliver Smithies in Physiology and Medicine for their work on ESC from mice using gene-targeting strategies producing genetically engineered mice (known as knockout mice) for gene research (42, 44).
In 2010 Xu *et al.* revealed the core signaling regulatory mechanism for pluripotent stem cell survival and self-renewal. In 2012, Nobel Prize for Medicine and Physiology was awarded to Dr. Yamanaka for creating induced pluripotent stem cells, and to Dr. John Gurdon who demonstrated early the adult cells have the genetic information to be pluripotent. In 2014, teams led by Dieter Egli and Young Gie Chung independently produced monkey embryonic stem cells from adult cells, using therapeutic cloning. Egli's team use skin cells from a woman with diabetes and demonstrate that the resulting stem cells can be turned into insulin-producing beta cells (42, 44). Hence, there are many alike reports of putative stem-cell-based treatments in genetic and degenerative disorders or severe injuries, however, the number of proven stem cell therapies still remain small.

1.1.5: Stem Cells in Medicine

Stem cells have great potential to become one of the most important aspects of medicine, as pluripotent stem cells give rise to the entire body of the organism. In some adult tissues, such as bone marrow, muscle, and brain, discrete populations of adult stem

cells generate replacements for cells that are lost through normal wear and tear, injury, or disease. In addition to the fact that they play a large role in developing restorative medicine, their study reveals much information about the complex events that happen during human development.

Many serious medical conditions, such as birth defects or cancer, are caused by improper differentiation or cell division. Currently, several stem cell therapies are possible, among which are treatments for spinal cord injury, heart failure(45), retinal and macular degeneration(46), tendon ruptures, and type 1 diabetes(47). Stem cell research can further help in better understanding cell physiology, human development and diseases and this may result in finding new ways of treating currently incurable diseases.

1.1.6: Stem Cell Microenvironment: The Niche

In vivo stem cells live in a complex microenvironment called the stem cell niche (Fig. 1.1.6(48)) (48, 49) and this niche influences cell behavior and regulates cell fate decisions by providing a variety of signals (50). These signals may be structural, physical, electrical, or biochemical. The stem cell niche typically constitutes stem cells, supporting cells, and the ECM. The ECM, the physical scaffold synthesized by cells, is involved in almost all of these signals. Cells elaborate their ECM by secreting proteins, and later, the ECM regulates cell behavior and influences the remodeling of their matrix. It's now widely accepted that ECM properties play a critical role in controlling stem cell fate. Such ECM properties include the protein composition of matrices, the availability of binding sites for specific integrin heterodimers, growth factor and cytokines, and physical properties like rigidity. Integrins, as a micro-environmental sensor, mediate interactions between stem/support cells and the surrounding ECM. The cell-ECM interactions are

critical for niche morphogenesis, anchorage of stem and support cells, positioning of dividing stem cells, and controlling the balance between stem cell renewal and differentiation (51, 52).

1.2: Cell Adhesion and Significance in Stem Cell Biology

The ability of a cell to adhere to other cells and to the surrounding extracellular matrix in a highly specific manner is essential to maintain integrity and order in multicellular organisms. Adherence provides fundamental cues to the cell to polarize, elaborate specific products, migrate to correct destinations, or make physiological barriers and cooperative tractions (2). This high specificity in cell adhesion is reflected in the multiplicity of cell adhesion molecules that a cell normally has and the variety of extracellular matrix molecules that the cell interacts with (53-55).

Several adhesion receptor supergene families have been described: integrins, cadherins, selectins, CD44 related molecules and transmembrane proteoglycans (53). Integrins are the major group of cell adhesion receptors that mediate attachment to the extracellular matrix and are the focus of this thesis.

1.2.1: Integrins and Their Structure

The name “integrin” was suggested for an integral membrane protein complex first characterized in 1986 (56). The name was devised because the protein identified linked the extracellular matrix to the cytoskeleton (early developments in this field have been well described (57).

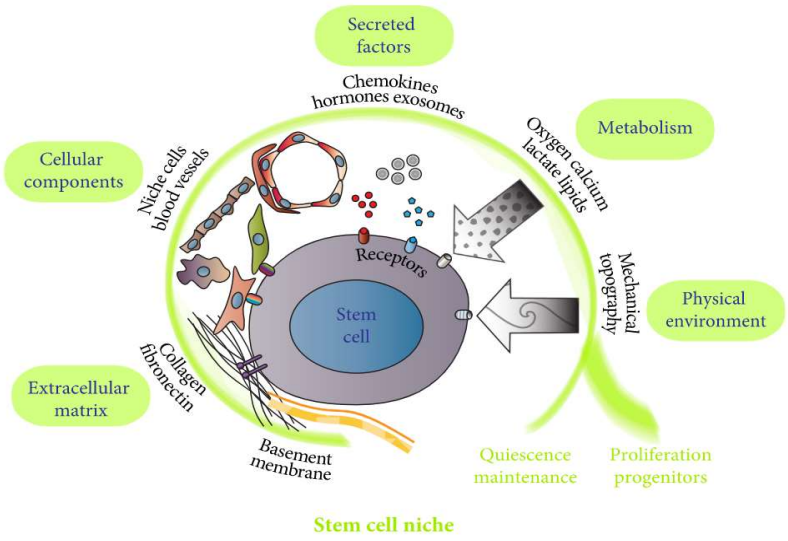

Figure 1.1.6: Schematic diagram of the stem cell niche. A stem cell and its interacting factors and components of the microenvironment known to regulate resident stem cells are shown. The actual niche architecture and components may vary for different types of embryonic, adult stem cells and progenitor cells. Not drawn to scale are examples of various cellular niche elements (fibroblasts, MSC, pericytes, endothelial cells, macrophages, tissue-specific niche architecture cells, and the interacting receptors); extracellular matrix (collagen, laminin, fibronectin, basement membrane, and the interacting integrins); secreted factors (exosomes, chemokines, hormones, and the signaling receptors); metabolism producing nutrients and redox state and their channels and transporters; and physical forces within the niche architecture and the corresponding mechanoreceptors.

The integrin family of adhesion molecules is drawing increasing attention as active regulators of stem cells. They are present in all nucleated cells, often in large numbers and many members can be expressed simultaneously in a given cell. Cells interact with ECM molecules via these surface receptor glycoproteins. The type and quantity of integrins on each cell are specific to the cell and tissue type. Integrins primary function is to facilitate the interactions between cells and ECM and transduce chemical and physical signals from the matrix. They are involved in many cellular functions, including cell cycle progression, cell adhesion, migration, survival and are also

responsible for the organization of the cytoskeleton and structural components of the ECM(58).

Integrins are heterodimeric transmembrane receptors composed of two glycoprotein subunits, α and β. In vertebrates, 18 α subunits and 8 β subunits have been found, and they can form at least 24 different heterodimeric structures. Each subunit has a large extracellular domain and short cytoplasmic fragment (50 amino acids, with the exception of β4 which is about 1000 amino acids) forming a typical type I transmembrane glycoprotein (4, 59, 60).

The extracellular domain of integrins binds to ECM ligands, such as laminin, fibronectin, collagen, and vitronectin, while the intracellular domain connects with cytoskeletal proteins, such as α-actinin and talin, as well as regulatory proteins, like calreticulin and cytohesin. Integrins interact with ligands through weak interactions, however, the ligand-binding affinity may be modulated by intracellular signals. In general, the ligand-binding domain of integrins is at the ends of integrins, and it has portions on both subunits. Once the ligand binds the two subunits, the induced conformational change physically pushes the two subunits apart and initiates downstream signaling. The binding between integrin receptors and ECM proteins is not specific. One ligand may interact with different integrin receptors, while one integrin may recognize different ligands. This transmembrane linker role makes integrins important in cell–cell/cell–ECM adhesion, signal transduction, and growth factor receptor responses (5, 61, 62).

Integrins communicate in both directions in a cell. In outside-in signaling, ligands bind to extracellular integrin domains, where a conformational change occurs so that the

signal is transmitted into the cell. Inside-out signaling originates from non-integrin cell surface receptors or cytoplasmic molecules and it activates signaling pathways inside the cells, ultimately resulting in the activation/deactivation of integrins. And here, adhesion may be regulated both by conformational changes in the integrin and by valency change (integrin clustering) (2).

In order to understand signaling dynamics, it is important to have a good knowledge of integrin structure. As described above, integrins are heterodimers of non-covalently associated α and β subunits. The α and β subunits are constructed from several domains with flexible linkers between them. Each subunit has a single membrane-spanning helix and, usually, a short unstructured cytoplasmic tail. The size varies but typically the α and β -subunits contain around 1000 and 750 amino acids, respectively (3, 58, 59).

Integrin α subunits

The α subunit is composed of a seven-bladed β-propeller, which is connected to a thigh, a calf-1, and a calf-2 domain, together forming the leg structure supporting the integrin head (Fig. 1.2.2)(58). The last three or four blades of the β-propeller contain EFhand domains that bind Ca^{2+} on the lower side of the blades facing away from the ligand-binding surface. Nine of the integrin α chains contain an I domain, also called the A domain, which is a domain of approximately 200 amino acids, inserted between blades 2 and 3 in the β-propeller. Ligand binding occurs via a coordinating Mg^{2+} ion in the metal-ion-dependent adhesion site (MIDAS) motif (63, 64).

Integrin β subunit

The β subunit contains a plexin-sempahorin-integrin (PSI) domain, a hybrid domain, a βI domain, and four cysteine-rich epidermal growth factor (EGF) repeats(65). The βI domain contains an Mg2+ coordinating MIDAS and a site adjacent to MIDAS (ADMIDAS) binding an inhibitory Ca2+ ion, and where binds the Mn2+ ion leading to a conformational change resulting in an active form of the integrin(64). The β integrin chains share homology in the cytoplasmic tail, with NPX/Y motifs able to bind proteins containing PTB domains, and several proteins were reported to interact with the β subunit. Talin 1–2 and kindlins 1–3 seem to act synergistically to activate integrins by binding to integrin β subunit tails, whereas filamin A negatively regulates activation. More recently, the integrin linked kinases (ILK) and focal adhesion kinase (FAK) enzymes taking part in outside-in signaling have also been shown to affect integrin activation via inside-out signaling (58, 66, 67).

1.2.2: Integrin Activation and Signaling

For the interaction of integrins with their ligands to be meaningful, the binding event must be able to regulate signal transduction. As integrins lack enzymatic activity, signaling is instead induced by the assembly of signaling complexes on the cytoplasmic face of the cell. Such signaling complexes are formed in two ways; first, by receptor clustering, which increases the avidity of molecular interactions thereby increasing the on-rate of binding of effector molecules, and second, by induction of conformational changes in receptors which creates or exposes effector binding sites, and this sort of regulation seems to be the primary mode of affinity regulation of integrins. This later demands a mechanism for conveying conformational changes between the cytoplasmic tails and the ligand-binding head domain over a relatively large distance (around 20 nm) (58).

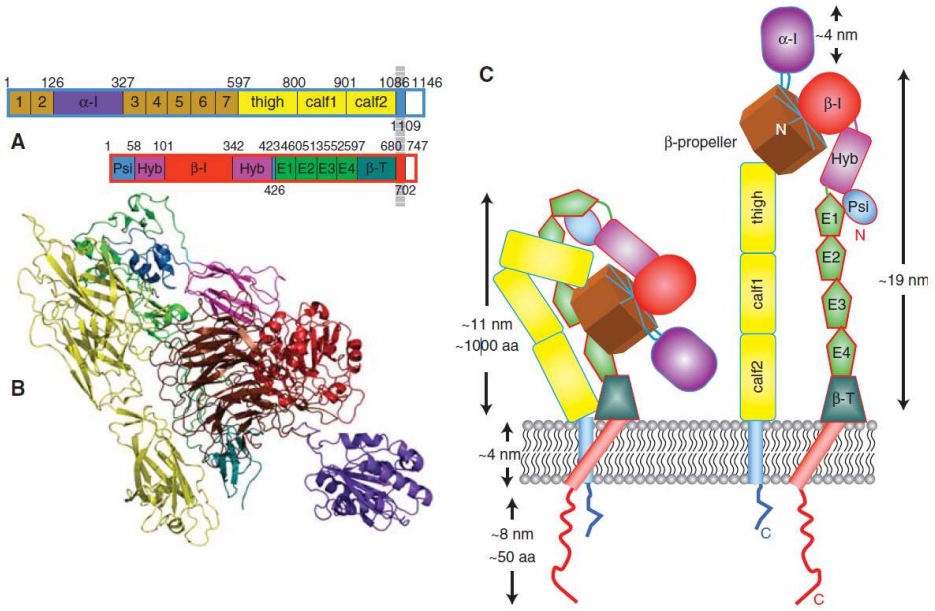

Figure 1.2.2. Integrin structure. A, Domain structure of αxβ2; B, structure of αxβ2 using same color code as A; C, cartoon representation of integrin conformations with approximate dimensions.

Integrins control cellular functions through inside-out and outside-in signaling including cell motility, survival, differentiation and proliferation (through interaction with members of the Cyclin family) as well as ECM remodeling and embryonic development.

The extracellular domain of integrins can bind ECM proteins used in ESC support such as collagen, fibronectin, laminin and vitronectin. Integrins can also associate with receptors on the surface of other cells through direct interaction with membrane bound proteins such as vascular- or intracellular- cell adhesion molecules (VCAM and ICAM) or through linker molecules such as von Willebrand factor, which assists in the binding of platelets to one another during blood clotting (67).

Outside-in signaling of integrin receptors through interactions with the ECM generates clustering of integrin heterodimers called focal adhesion sites. Integrin clustering occurs after ECM adhesion promoting lateral association with other cell surface receptors and increases in the cytoplasmic concentration of cell signaling molecules such as PI3-kinase and MEK-ERK, which are already implicated in human ESC maintenance. The focal adhesion sites can recruit over 50 different cytoplasmic proteins to the integrin cytoplasmic domain, and comprise of 3 general classes: 1) integrin binding proteins (e.g. talin or focal adhesion kinase), 2) scaffold and adaptor proteins (e.g. those of the cytoskeleton, tensin, vinculin, paxillin and α-actinin) and 3) enzymes that effect downstream signaling to influence cytoskeletal remodeling, cell migration, survival and gene regulation (e.g. tyrosine kinases, serine/threonine kinases, tyrosine phosphatases) (68, 69).

1.2.3: Stem Cell Self-Renewal

Stem cell self-renewal is the process by which a mother stem cell divides symmetrically or asymmetrically to generate at least one daughter cell, which retains a developmental potential similar to the mother stem cell. The ability of stem cells to divide asymmetrically to produce one stem and one non-stem daughter cell is often considered to be one of the defining characteristics of stemness. Stem cells are capable of two types of symmetric divisions: a proliferation division resulting in the creation of two stem cells, and a differentiation division resulting in the creation of two differentiated cells (70).

The ability to self-renew is essential for stem cells to expand their numbers during development, to be maintained within adult tissues, and to restore the stem cell pool after injury. Defects in self-renewal mechanisms can lead to developmental defects, premature aging phenotypes, and cancer (71). Hence, the elucidation of self-renewal mechanisms offers the potential for fundamental insights into development, cancer, and aging.

Stem cell self-renewal requires mechanisms that confer the ability to divide while remaining undifferentiated. In the case of ESC, the self-renewal potential which is conferred by unique transcriptional regulation (marked by an OCT4-SOX2-NANOG transcriptional network) as well as unusual cell cycle regulation (marked by a very short and relatively unregulated G1 phase). The self-renewal of tissue-specific stem cells is mitogen dependent, and mechanisms regulating the G1-S transition, including the $p16^{Ink4a}$-Rb and $p19^{Arf}$-p53 pathways, govern quiescence versus activation (72). On the other hand, the maintenance of self-renewal in tissue stem cells is achieved by inhibiting the expression or function of lineage-specification genes, by asymmetrically segregating their gene products into differentiating daughter cells, or by balancing the activities of mutually inhibitory lineage specification gene products. The long-term self-renewal ability of tissue stem cells depends on mechanisms that maintain their genomic integrity, such as those involved in ROS detoxification, telomere maintenance, and DNA damage repair. Tissue stem cell self-renewal also depends on cell-extrinsic regulation. The niche provides stem cells with physical anchorage as well as membrane-bound and secreted factors that regulate survival, polarity, quiescence, and differentiation. Long-range signals dynamically modulate stem cell activity according to physiological demands. Tissue stem cells undergo changes in self-renewal potential, developmental potential, and

cell cycle status at different stages of life, in response to changing developmental and regenerative demands. These changes require stem cells to employ distinct self-renewal programs at different stages of life. Self-renewal programs involve networks that balance proto-oncogenes (which promote self-renewal), gate-keeping tumor suppressors (which limit self-renewal), and care-taking tumor suppressors (which maintain genomic integrity) (70).

More importantly, before stem cell-based therapies are applied in clinics, a fundamental issue needs to be elucidated to gain a precise control over stem cells response, in terms of self-renewal and differentiation. Specifically, a broader understanding of the interplay between stem cells, their niche, and external forces that can aid in either self-renewal or differentiation of stem cells, is currently lacking.

1.2.4: Integrin Signaling on Human Pluripotent Stem Cells Self-Renewal

Molecular mechanisms for hPSC self-renewal have been recently started to be uncovered. Generally, integrins transmit their signals via intracellular signaling proteins, such as ILK and FAK (73). ILK was shown to mediate integrin signals to AKT signaling pathway, and this signaling pathway had an antagonistic effect on endoderm differentiation, and thus promoting self-renewal and survival of hPSC (74-76). On the other hand, a recent study showed that the integrin-FAK signaling pathway was not active in undifferentiated hPSC, and was localized in the nuclei of hPSC, interacting with OCT4and SOX2. During differentiation, however, integrin α6 levels diminished, and FAK became active (or phosphorylated at Y397) (61). Taken together, the integrin-ILK signaling pathway is active in order to maintain hPSC self-renewal and survival through

the activation of AKT signaling pathways, and the integrin-FAK signaling pathway is inactive.

1.2.5: Integrin α6 in Stem Cell-Niche Interaction and Self-Renewal

The ability of stem cells to reside in the niche for a long period of time is paramount for tissue homeostasis and regeneration. A6-Integrin-mediated ECM adhesion is critical for anchorage and long-term maintenance of a variety of stem cell populations in the niche. Disruption of interactions between α6β1 and laminin in the lateral ventricle of mice causes the release of neural stem cells (NSCs) in the sub-ventricular zone and activation of NSCs (26). Studies also support that α6β1 integrins play vital role in anchoring spermatogonial stem cells (10) and hematopoietic stem cells (77), and α6(β4) in anchoring dermal stem cells (78) to their niches.

In breast cancer, α6(β1) expression promotes self-renewal of tumor-initiating cells (TICs) and mediates transduction of cell signals essential for establishment of an autocrine loop to maintain the TIC niche (19). Deletion of α6β1 results in random orientation of the basal cell division plane and impairs epithelial homeostasis (79). Furthermore, laminin511 (LM511) engagement of α6β1 supports the self-renewal of mouse ESC, whereas internalization of α6β1 promotes mESC differentiation towards an epithelial lineage via a FAK/Akt/Erk-dependent mechanism (80, 81).

Currently, there is limited information for the role of α6 cytoplasmic variants in the regulation of stem cell–niche interactions. $CD34^+$ and $CD34^+CD38^-$ bone marrow stem/progenitor cells express both α6A and α6B. Although α6A and α6B are equally associated with the β1 subunit and also have similar specificity and affinity for ligand binding, it was reported that only α6A(β1) was responsible for protein kinase C-

dependent activation of MAP kinases. Also, α6A(β1) was found to be more active than α6B(β1) in promoting migration of bone marrow stem cells.

1.3: *In-Vitro* Culture of Human Pluripotent Stem Cells

The growth and advancement in the applications of hESC/hiPSC technology have been accompanied by a huge body of work dedicated to optimizing and standardizing hPSC culture. Optimization of culture systems is not only limited to defining culture media components but also the extracellular matrices, environmental cues, and modes of passaging, which has led to the development of simple and defined culture conditions and also facilitated the development of 3D and bulk cell culture systems. Chemically defined media are ideal for minimizing lot-to-lot variation and ensure consistency, for both research-based and clinical applications, while xeno-free and cGMP-compliant culture systems are preferred for cellular transplantation. Efforts in this direction have largely focused on understanding the signaling molecules required, replacing nonhuman components of media and developing synthetic substrates, which have an immediate application in disease modelling and can eventually be used to engineer cells and their substrates for therapeutic applications. Most of the commercially available media formulations consists of a core of three major signaling components: 1) insulin or insulin growth factor (IGF1), that bind INSR and IGF1R to signal the PI3K/AKT pathway promoting survival and growth; 2) FGF2 and/or neuregulin 1 (NRG1), that bind FGFR1/FGFR4 or ERBB3/ERBB4, respectively, activating the PI3K/AKT/mTOR and MAPK/ERK pathways; and 3) TGF-β1, NODAL, or Activin A, that bind TGFBR1/2 and/or ACVR2A/2B/1B/1C to activate the TGF-β signaling pathway.

Multidisciplinary approaches are available for the derivation and culture of different stages of pluripotency, development of xeno-free culture conditions as well as the generation of GMP-compatible protocols. The derivation and maintenance hPSC have to be done in a manner that recapitulates their equivalent niche in vivo, suggesting that the media in which these cells are cultured in are central to the success of all downstream applications and their use in stem cell engineering.

1.4: Obstacles in Stem Cell Biology

Revolutionary scientific and medical advances always have to be carefully policed in order to make sure they are both ethical and safe. Because stem cell therapy already has a large impact on many aspects of life, it should not be treated differently. Currently, there are several challenges concerning stem cells. First, the most important ones are about fully understanding the mechanisms regulating stem cells fate. The efficiency of stem cell-directed differentiation must be improved to make stem cells more reliable and trustworthy for a regular patient. Future stem cell therapies may be a significant obstacle and will require interdisciplinary collaboration. The identification and proper isolation of stem cells from a patient's tissues is another challenge. Immunological rejection is a major barrier to successful stem cell transplantation. Although these challenges facing stem cell science can be overwhelming, the field is making great advances each day. Stem cell therapy is already available for treating several diseases and conditions. Hence, considering stem cell therapy and all regenerative benefits their impact on future medicine appears to be highly significant.

CHAPTER TWO

MATERIALS AND METHODOLOGY

2.1: Preparation of Matrigel-Coated Plates

Matrigel (BD BioSciences, NJ, USA) was diluted to a concentration of 0.1 mg/ml in cold Dulbecco's modified Eagle's medium/F12 (DMEM/F12; GIBCO) and then applied to TCPS dishes. The coating was allowed to polymerize during 2 h incubation at room temperature. Before plating cells, excess Matrigel-DMEM/F12 solution was aspirated and the dishes were washed with sterilized D-PBS.

2.2: Synthetic Surface Preparation on TCPS

The UVO-initiated free radical polymerization was carried out in a fume hood with connections for nitrogen gas. Each reaction was used to prepare 24 TCPS, and this procedure was reproducible repeated 10 times producing 240 PMEDSAH-grafted plates. The monomer solution consisting of 0.25 M MEDSAH was dissolved in a mixture of deionized water and ethanol (4:1, v/v) in a 500 mL reaction vessel. The solution was degassed for 60 min by nitrogen purge. Then, the monomer solution was heated to 70-72^{0}C. While the reaction vessel was being heated, TCPS plates were activated by UV ozone treatment for 40 min to create initiation sites on the surface. After activation, the plates were transferred to the reaction vessel and the temperature was raised to 76-80^{0}C. The surface-initiated polymerization occurred over a 2 h time period under nitrogen atmosphere at 76-80^{0}C. Once the process was complete, grafted plates were removed from the reaction vessel and were rinsed with 1% saline (w/v) solution at 50^{0}C, followed by ultra-sonication in DI-water and air drying inside the hood.

2.3: Preparation and Use Of 10% Human Serum (HS) Treated (HSt)-PMEDSAH Grafted Plates.

Freshly prepared PMEDSAH grafted plates were treated with 10% HS (v/v DMEM/F12) 10% for 30 minutes at room temperature, followed by couple washes with cold D-PBS.

Two sets of 10% HSt-PMEDSAH plates were prepared. The first set was used right after its preparation for culturing hESC for 20 consecutive passages. For the other set of 10% HSt-PMEDSAH plates, after their wash with cold sterilized Dulbecco's phosphate buffered saline (D-PBS), the plates were air dried and wrapped with parafilm and stored at 4^0C until their use for cell culture and were sued for weekly passaging of hESC until passage 13. In both conditions, after 5 passages the cells were characterized for self-renewal and pluripotency.

2.4: Preparation of Microgravity Chamber Slides and Cell Culture Substrate

Microgravity chambers were prepared inside Clipmax chamber-slides flasks (TPP Techno Plastic Products AG, Switzerland), in which a small culture channel was created with polydimethylsiloxane (PDMS), as described before (82). Briefly, a 1:10 (w/w, curing agent: base monomer) ratio PDMS pre-polymer (Sylgard 184, Dow-Corning, Midland, MI) was poured over the two sides and on the top of the Clipmax chamber-slides flasks, and cured at room temperature for 12 hours each side, leaving the bottom of the chamber without PDMS (Fig. 1A). The ug chambers have an approximate dimension of 10 x 60 mm, and align to the rotation axis (Fig. 3.2B). Matrigel (BD BioSciences, San Jose, CA) was diluted to a concentration of 100 µg/ml in cold DMEM/F12 (Gibco Life Technologies, Waltham, MA) and then applied to the bottom of the ug chamber. The

coating was allowed to polymerize during 2 hours incubation at room temperature(12). Before plating cells, excess Matrigel-DMEM/F12 solution was aspirated, and chambers were washed with Dulbecco's phosphate buffered saline (D-PBS) (Gibco Life Technologies).

2.5: Simulated Microgravity (sμg)

A clinostat rotator was developed following a previous report (83) to create 2-D sμg conditions for adherent cells. Cells were seeded on the ug chambers and located in close proximity to the rotation axis, where they were exposed to minimal centripetal forces at a speed of 80 rpm and experienced simulated chronic free fall. The magnitude of ug spans from ≤0.012g to ≤0.034g, depending on the location of cells in relation to the rotation axis, as reported previously (83) (Fig. 3.2B). Two ug chambers were placed back-to-back on a custom-designed holder that was 3D printed using ABS plastic (Fig. 3.2C). The holder was connected to a Multi-purpose Tube Rotator (Fisherbrand, Ontario, Canada). The instrument holding the two ug chambers was placed inside of a dedicated cell culture incubator set up at 37°C, 95% humidity and 5% CO_2 conditions (Fig. 3.2D). As a control, cells were cultured in ug chambers in static 1g conditions for the same period of time (Fig. 3.2E).

2.6: Cell Culture

2.6.1: Cell Culture, Evaluation of Pluripotency and Induced Differentiation of Human Pluripotent Stem Cells (hPSC)

All experiments were repeated at least in triplicates with NIH-approved hESC H1 and H9 (WiCell Research Institute Inc., Madison, WI) and hPSC derived in our laboratory. The undifferentiated hPSC were cultured on Matrigel coated tissue culture

plates (Applied Biosystems, Foster City, CA) with StemFlex Medium (Gibco Life Technologies) and maintained in cell culture incubators with high humidity and 5% CO_2 at 37°C. For experimental conditions in ug chambers, hPSC were dissociated into single cells using L7 dissociation solution (Lonza, Basel, Switzerland) and 10,000 cells were plated on Matrigel coated ug chambers completely filled with StemFlex medium and 10 µM of ROCK inhibitor (Stem Cell Technology, Vancouver, Canada) (84). Twenty-four hours post-seeding, two ug chambers were transferred to sµg condition, while the other remaining two ug chambers were assigned as control group and were cultured at 1g in static conditions. The culture medium was replaced every other day. Human foreskin fibroblasts (hFF; ATCC) were cultured in similar conditions with α-MEM medium supplemented with 10% fetal bovine serum (FBS).

In-vitro analysis of pluripotency of hPSC from each group was evaluated by embryoid body (EB) formation. Cells were cultured in suspension with DMEM (Gibco Life Technologies) supplemented with 10% FBS for 10 days. Direct differentiation of hPSC was performed on ug chambers with chemically defined medium (CDM) consisting of DMEM/F12 (Gibco Life Technologies) supplemented with 1 × N2 (Invitrogen), 1 × B27 (Invitrogen), 0.11 mM 2-mercaptoethanol, 1 mM nonessential amino acids (Gibco Life Technologies), 2 mM L-glutamine (Gibco Life Technologies), and 0.5 mg/ml bovine serum albumin (BSA) (fraction V; Sigma-Aldrich) for 4 days following established protocols (85). To induce trophectoderm differentiation, cells were cultured in CDM supplemented with 50 ng/ml human recombinant bone morphogenetic protein (BMP) 4 (Stemgent, Cambridge, MA) and in CDM supplemented with 4.5 µM retinoic acid (RA) (Stemgent) to induce neuro-ectoderm differentiation.

In addition, formation of EB from hESC passage 20 cultured on 10% HSt-PMEDSAH plates was done using cell clusters cultured in suspension in 10% FBS/DMEM alpha (Life Technologies) on ultra-low cell attachment dishes (Corning) for 10 days to promote differentiation. Quantitative analysis of self-renewal and pluripotency assessed by the trilineage differentiation potential of hESC cultured on 10% HSt-PMEDSAH plates at passage 20 was done using TaqMan hPSC Scorecard Assay (Thermo Scientific) following the manufacturer's protocol. Briefly, total RNA from undifferentiated hESC cultured on 10% HSt-PMEDSAH plates and EB obtained from same pool of hESC was extracted and used to generate respective cDNA as described above. Respective cDNA samples, TaqMan Fast Advanced Master Mix Template and RNase-free water were combined and reconstituted in each well of two 96-well plates contains 94 predefined TaqMan Gene Expression assays (including endogenous controls) dried-down in the wells TaqMan® hPSC Scorecard™ Panel by adding 10 µL of the reaction mixture per well. Each plate was loaded and run using StepOnePlus Real-Time PCR System (Thermo Scientific) with the fast thermal cycling condition. The gene expression data was analyzed using the web-based hPSC Scorecard™ Analysis Software to confirm the pluripotency of the samples and predict their differentiation potential and outcome by comparing to a common reference set.

2.6.2: Derivation, Culture and Characterization of MSC

To induce differentiation of iPSC into MSC, embryoid bodies (EB) were formed and cultured in suspension for 7 days with hCCM in low-attachment culture dishes. Approximately 70 EB were plated onto 0.1% gelatin-coated dishes in growth medium (alpha minimum essential medium: α-MEM, 10% fetal bovine serum: (FBS), 200 mM L-

glutamine and 10 mM NEAA). Cells growing from these EB were cultured for up to 2 weeks to reach confluence and passaged until a homogeneous fibroblastic morphology appeared. In subsequent culture, cells were seeded at a density of $7 \times 10^3/cm^2$.

2.6.3: Cell Doubling Time

The cell doubling time was calculated using the algorithm provided by http://www.doubling-time.com/compute.php, with an initial seeding of 7×10^3 cells per well and evaluated at 6, 24, and 48 hours post-seeding. The assay was performed in triplicate.

2.7: Quantitative Analysis of Undifferentiated Colony Size and Total Number of Cells

Microscopic images of undifferentiated hPSC colonies were used to calculate the colony area of at least 10 randomly selected colonies after 96 hours of culture under sμg and 1g conditions using NIH ImageJ software (http://rsb.nih.gov/ij). Data from independent replicates were averaged and standard deviations were calculated, compared, and used for statistical analysis. The total number of cells after 96 hours of culture under sμg and 1g conditions was calculated after dissociation of colonies into single cells and counted using a hemocytometer.

In addition, during 5 initial and consecutive weekly passages the total number of cells grown on each plate of 10% HSt-PMEDSAH and Matrigel was counted and recorded at the time of passage for comparative analysis. From the total number of cells obtained, 10,000 cells were used per passages into a new substrate. A theoretical yield of total cell number of hESC obtained on different substrates was calculated assuming that all cells would be passaged each week instead of the only 10,000 single cells that were seeded. The theoretical yield of cells was determined with the formula $CN_{(n+1)} = CN_n \times$

$TN_{(n+1)}/20{,}000$, in which CN is the calculated total cell number, TN is the total cell number and *n* is the passage number.

2.8: MSC Differentiation Assays and Alkaline Phosphatase Staining

For functional differentiation, MSC at passages 6 and 7 were used. For osteogenesis, cells were incubated in α-MEM with 10% fetal calf serum (FCS), 100 U/ml penicillin, 100 µg/ml streptomycin, 2 mM L-glutamine, 10 mM β-glycerophosphate (Sigma), 100 nM dexamethasone (Sigma), and 50 µM ascorbate-2-phosphate (Sigma). Media were changed two times per week for 3 weeks. Cells were fixed with 10% formalin for 20 minutes at RT and stained with Alizarin Red, pH 4.1 for 20 minutes at RT.

For adipogenesis, cells were incubated in DMEM with 15% fetal calf serum (FCS), 100 U/ml penicillin, 100 µg/ml streptomycin, 12 mM L-glutamine, 5 µg/ml insulin (Sigma), 50 µM indomethacin (Sigma), 1×10^{-6} M dexamethasone (Sigma), and 0.5 µM 3-isobutyl-1-methylxanthine (Sigma). Media were changed two times per week for 3 weeks. Cells were fixed with 10% formalin for 20 minutes at RT and stained with Oil Red (Sigma) in ethanol for 20 minutes at RT.

Chondrogenic differentiation was induced by culturing 2×10^6 iPS-MSC in pellets. Cells were suspended in 2 ml of chondrogenic medium in 15 ml centrifugation tubes and centrifuged at 600*g* for 5 minutes and cultured for 21 days. Medium was changed every 3 days and consisted of high-glucose DMEM (Gibco; Grand Island, NY; http://www.invitrogen.com) with 10% FBS (Gibco), 100 mM sodium pyruvate, 40 µg/ml proline, 100 nM dexamethasone, 200 µM ascorbic acid (all from Sigma), and 10 ng/ml transforming growth factor (TGF)-β3 (R&D systems; Minneapolis, MN;

http://www.RnDSystem.com). Cells were fixed with 10% formalin for 20 minutes at RT and stained Safranin O (Sigma) in ethanol for 20 minutes at RT.

Undifferentiated colonies were identified by specific alkaline phosphatase staining, which was done using the Alkaline Phosphatase Staining Kit (Stemgent). Briefly, cells were fixed with fixing solution for 2-5 minutes, then rinsed and incubated in AP Substrate Solution in the dark at room temperature for 15 minutes. Cells were rinsed and covered with 1 × PBS to prevent drying before quantitative analysis.

2.9: Immunofluorescence Staining

Cells grown on 10% HSt-PMEDSAH plates were fixed in 4% paraformaldehyde for 15 min at room temperature and then permeabilized with 0.1% Triton X-100 for 10 min. Primary antibodies raised against OCT3/4 (Cell signaling), SOX2 (Millipore), NANOG (Abcam), TRA 1-60 (Abcam), TRA 1-81 (Millipore) were diluted in 1% normal serum and incubated overnight at 4^0C, and detected with respective secondary antibodies. Micrographs were captured using an EVOS®FL Cell Imaging System (Thermo Scientific).

2.10: Flow Cytometry Analysis

Cells were washed with PBS and harvested by incubation in L7 hPSC passaging solution. After this, cells were incubated for 30 minutes in dark at 4^0C first with human IgG to block un-specific binding and then with human/mouse NANOG APC-conjugated antibody (Biolegend), OCT4PE-conjugated antibody (Biolegend), SSEA3 APC-conjugated antibody (R&D systems), SSEA4 PE-conjugated antibody (R&D systems), TRA 1-60 FITC-conjugated antibody (Biolegend), TRA 1-81 PE-conjugated antibody (Biolegend), NANOG. At least 10,000 events were acquired for each sample using a BD

FACSCanto II (BD Biosciences) and flow cytometry data were analyzed using FlowJo software (https://www.flowjo.com/).

2.11: RNA Isolation and Quantitative Real-Time PCR and Reverse Transcription PCR

Total RNA was extracted using TRIzol (Invitrogen, Carlsbad, CA) and purified using RNeasy Mini Kit (Qiagen, Hilden, Germany) and DNase I treatment. The yield and purity of RNA was estimated spectrophotometrically using the A_{260}/A_{280} ratio. One ug of total RNA was reverse transcribed into cDNA using Superscript III Reverse Transcriptase (Invitrogen) and the equivalent of 10 ng was used for PCR. These reactions were carried out in a final volume of 20 µL containing 0.2 mM deoxynucleotide triphosphates, 120 nM of each primer, and 1 U Taq-DNA-polymerase. The Taqman probes used are listed in Supplementary Table 1. Gene expression was determined by quantitative real-time PCR on an ABI Prism 7700 Sequence Detection System (Applied Biosystems). The relative RNA expression levels of target genes were analyzed by the comparative $\Delta\Delta C_T$ method (86) using *GAPDH* as an internal control. Subsequently, expression levels of the investigated genes were normalized to expression levels of control samples and reported as fold changes. Changes larger than 2-fold in relative mRNA expression were considered significant. The Taqman human cyclins and cell cycle regulation gene array (Applied Biosystems; Waltham, MA) was used following the company protocol.

For reverse transcription PCR, 1 µg of total RNA was reverse transcribed using SuperScript™ One-Step RT-PCR with Platinum® Taq (Invitrogen). The primer sequences for *KI67* are for forward: TTGTGCCTTCACTTCCACAT and for reverse: CTGGTAATGCACACTCCACCT, while for *TBP* forward:

CTCCCACCCAAAGTCTGATGA and reverse: GCCATAAACCAAGCAGGACG. The cDNA synthesis and pre-denaturation were carried out at 95°C for 2 minutes. PCR amplification was performed for 35 cycles at 95°C for 30 seconds, 55°C for 30 seconds and 72°C for 30 seconds. The final extension cycle was run at 72°C for 10 minutes. Finally, 14 μL of PCR product was loaded onto a 1.0% agarose gel. Band densitometry analysis was performed using ImageLab 6.0 (Bio-Rad, Hercules, CA, USA).

2.12: Western Blot Analysis

The following antibodies were used: OCT4 (Santa Cruz Biotechnology), NANOG (Cell Signaling Technology), SOX2 (Cell Signaling Technology), Integrin α6 (Millipore), Integrin β1 (Santa Cruz Biotechnology), PSMD11 (Novus Biologicals; Centennial, CO) and GAPDH (Cell Signaling Technology). Whole cell lysates were prepared from cells, separated on 10% SDS-polyacrylamide gel, and transferred to polyvinylidene difluoride membranes. The membranes were incubated with 5% milk in TBST (w/v) for 1 hour and then incubated with primary antibodies diluted in 5% BSA in TBST overnight at 4°C. Blots were incubated with horseradish peroxidase-coupled secondary antibodies (Promega, Madison, WI; R&D systems, MCKInley NE, MN) for 1 hour, and protein expression was detected using SuperSignal West Pico Chemiluminescent Substrate or SuperSignal West Femto Chemiluminescent Substrate (Thermo Scientific, Waltham, MA). NIH ImageJ software was used for quantification of Western blot images.

2.13: Reprogramming of Human Somatic Cells into iPSC on 10% Hst-PMEDSAH Dishes and Quantification of Reprogramming Efficiency

For iPSC reprogramming, 3 x 10^5 human gingival fibroblasts (hGF) were seeded on a 10% HSt-PMEDSAH plate in high-glucose DMEM supplemented with 10% Human Serum (HS; Sigma), 1% nonessential amino acids (NEAA) (Gibco Life Technologies), 1% GlutaMax (Gibco Life Technologies), and 1% penicillin streptomycin (Gibco Life Technologies). When cell confluence reached about 50%, the Sendai viral vectors carrying KLF4, SOX2, OCT3/4, and c-MYC (CytoTune kit 2.0, ThermoFisher Scientific) supplemented with 10 μg of hexadimethrine bromide (Polybrene; Sigma-Aldrich) was used for reprogramming into iPSC using standard protocols. Eight hours later, fresh medium was added. Seventy-two hours later, cells were subcultured into six 10% HSt-PMEDSAH plates and then twenty-four hours later the medium was replace with StemFlex medium (Thermo Scientific) supplemented with 10 μM Y-27632 dihydrochloride (Stem Cell Technologies, Vancouver, CA). The hPSC culture medium with ROCK inhibitor was refreshed every day until week 3 or 4 until iPSC colonies appeared. The human iPSC colonies were analyzed by alkaline phosphatase (AP) activity, and together with colony morphology (well defined borders and high nuclei per cytoplasmic ratio) was used to identify reprogrammed hiPSC colonies. The number of hiPSC colonies obtained on 10% HSt-PMEDSAH plates and Matrigel coated plates were quantified and used to calculate the respective reprogramming efficiency as follows: the number of hiPSC colonies in each group was divided by 3×10^5, which was the original number of fibroblasts plated for each group before reprogramming. In addition, the human iPSC were further characterized for self-renewal and pluripotency potential by immunostaining, flow cytometry, and qPCR analysis.

2.14: Cytogenetic Evaluation

After 20 weeks of cell culture, standard G-band analysis (Karyotype analysis) on was performed on cells cultured on 10% HSt-PMEDSAH dishes by a cytogenetic specialist at the WiCell Institute (Madison, WI). Chromosomes were prepared using standard protocols and measurements were performed using Giemsa/Trypsin/Leishman (GTL) -banding method on at least 20 metaphase preparations.

2.15: RNA Sequencing

Total RNA (>500 ng with RIN >7.0) was used to prepare TruSeq Stranded mRNA library using the TruSeq Stranded mRNA LT Sample Prep Kit following manufacturer's library preparation protocol (TruSeq Stranded mRNA Sample Preparation Guide, Part #15031047 Rev. E). Whole transcriptome sequencing for six samples (three sμg and three matched control samples) were performed using Illumina NovaSeq6000 S4 sequencer. More than 100 million 2x151 pair-end reads were generated per sample with phred quality score Q30 > 90%. In order to test the robustness of the RNA-seq gene expression quantification results with respect to different bioinformatics pipelines, we generated five versions of raw counts matrices using several pipelines with different parameter settings. First, RNA-seq reads were aligned to GRCh38.p13 (GENCODE release 36, www.gencodegenes.org/human) using STAR (2.7.7a) with default parameters. In addition, we changed the default parameters *outFilterScoreMinOverLread* and *outFilterMatchNMinOverLread* from 0.66 to 0.30 and generated a second-version of alignment. Both RSEM (v1.3.3) and Salmon (1.4.0) were used to quantify the gene expression with their default parameters using the two versions of STAR alignments, resulting in four versions of the gene expression raw count matrices. In addition, Salmon

was used in mapping-based mode (without using STAR alignments) to generate the fifth version of gene expression raw count matrices. The fifth version of gene expression results was highly consistent with each other (Supplementary. Fig. 6). DESeq2 (1.30.0) was used to perform differential gene expression analysis using all five versions of the gene expression results. GSEA (v4.1.0) was used to perform gene set enrichment analysis.

2.16: Data Analysis

Three independent replicates for each experiment were performed and data were expressed as mean value ± SD. Two data sets were compared using unpaired student *t*-test function to calculate *p* values. Levels of statistical significance were set at $p < 0.05$. Asterisk denotes statistically significant differences (* = $P < 0.05$, ** = $P < 0.005$ and *** = $P < 0.0005$) detected by Student *t*- test.

CHAPTER THREE

EXPERIMENTAL RESULTS

3.1: Optimization and Standardization of Growth and Culture Conditions to Study hPSC

To successfully utilize hPSC in regenerative medicine and drug development, the culture methods must be improved to meet the technological standards in safety, cost-effectiveness, and the easiness of handling. Recently, large efforts have been made to formulate defined and xenogeneic-free culture media and extracellular matrices. We have already reported the first fully defined synthetic polymer coating (PMEDSAH) which maintained long-term growth of hESC. Here, we aim to optimize the preparation and use of this synthetic substrate coating to get better growth and maintenance of hESC as compared to other standard protocols.

3.1.1: Optimization and Standardization of PMEDSAH Grafting and hPSC Culture

We synthesized PMEDSAH grafted TCPS using surface-initiated graft polymerization procedure through optimization into one day protocol as described in details under the methods section (Fig. 3.1and 3.1.1). In an attempt to standardize the hPSC culture conditions on the chemically inert synthetic polymer coated TCPS using defined and xeno-free conditions, we did a systematic study to optimized cell attachment, and maintain long-term culture and self-renewal of hPSC. Our systematic study and analysis included the activation of integrins using the peptide (QHREDGS) (87, 88) or the integrin activating antibody (89, 90); by altering the pH of the media as suggested and supported by previous publications (91, 92), supplementing divalent cations and certain cytokines to the media to activate cell-ECM adhesion signaling (93-97), in addition to

treating (pre-conditioning) the freshly prepared PMEDSAH grafted (PMEDSAH-g) dishes with graded concentrations (1%, 10% and 100%) of fetal bovine serum (FBS) (98), Knockout™ Serum Replacement (KOSR) (12), and human serum (HS) (99, 100) (Table 3.1). Among all the treatments on the PMEDSAH-g dishes, and the supplements in chemically defined media (Table 3.1), pre-conditioned of the PMEDSAH-g dishes with 10% human serum (10% HSt-PMEDSAH-g) in DMEM/F12 for 30 minutes at room temperature followed by couple washes with cold PBS produced the following results in hPSC culture: improved cell attachment and long-term culture (until 20 consecutive passages) in an undifferentiated state, while retaining pluripotency as demonstrated by the ability to differentiate into endoderm, ectoderm and mesoderm derivatives; and maintaining a normal karyotype (Fig. 3.1.3). The 10% HSt-PMEDSAH-g dishes were tested on freshly prepared dishes and also on 10% HSt-PMEDSAH-g dishes which were prepared following the same protocol but stored at 4^0C in dried conditions for future use for weekly passage. On the other hand, we were not able to get stable attachment and growth of hPSC on PMEDSAH-g dishes using media supplemented with other graded concentration of HS. Our findings also indicate that treatment of TCPS with HS did not support stable attachment and growth of hPSC as observed in 10% HSt-PMEDSAH-g dishes (Fig. 3.1.3).

3.1.2: Culture and Expansion of hPSC on 10% HSt-PMEDSAH-g Dishes

We cultured hPSC on freshly prepared 10% HSt-PMEDSAH-g dishes and tested until passage 20, and also on 10% HSt-PMEDSAH-g dishes which were prepared in lots and stored at 4^0C for weakly passaging, and tested until passage 13.

Undifferentiated hPSC colonies were identified by observing colonies with compact morphology and defined border and by using alkaline phosphatase staining (101). Interestingly, at initial experiments the number of undifferentiated colonies and the total cell number (ratio) was higher on 10% HSt-PMEDSAH-g when compared to the Matrigel control group (Fig. 3.1.2A,B), but was not statistically significant.

To quantify the impact of synthetic polymer coatings and HS pre-conditioning, on attachment and long-term expansion of hPSC, a constant number (10,000) of hPSC cultured initially as single cells on Matrigel, and on 10% HSt-PMEDSAH-g dishes were done passaging weekly for five consecutive weeks. Attachment and growth of hPSC was observed to be better on 10% HSt-PMEDSAH-g dishes compared to the control group as shown in the micrographs in Fig. 2C. We calculated the hypothetical yield of total hPSC potential obtained after five passages on Matrigel and 10% HSt-PMEDSAH-g dishes assuming that all cells at each passage were sub-cultured, instead of the 10,000 cells that were actually propagated. It was estimated that on 10% HSt-PMEDSAH-g dishes, the expansion of 10,000 cells over a period of five weeks would yield up to 4.9×10^8 undifferentiated stem cells. This level of hPSC expansion on 10% HSt-PMEDSAH-g dishes was 2.1-fold greater ($p<0.0001$) than the theoretical yield calculated when cultured on Matrigel coated dishes as indicated in the graph in Fig. 3.1.2C. These calculated total cell numbers demonstrated that 10% HSt-PMEDSAH-g significantly facilitated the attachment and long-term growth and expansion of hPSC.

3.1.3: Characterization of hPSC Cultured on 10% HSt-PMEDSAH-G Dishes

The hPSC cultured on 10% HSt-PMEDSAH-g dishes were characterized for self-renewal and pluripotency, and also observed for genomic stability. Immunofluorescence

staining and flow cytometry analysis were performed to characterize the hPSC cultured on 10% HSt-PMEDSAH-g dishes. Colonies of hPSC cultured on freshly prepared 10% HSt-PMEDSAH-g dishes were observed to be strongly positive for several human self-renewal markers including NANOG, OCT4, SOX2, TRA 1-60 and TRA 1-81 as shown by the immunofluorescence staining micrographs on different passages (Fig. 3.1.3A). The hPSC were strongly positive when co-stained with SSEA3/OCT4 and SSEA4/OCT4as revealed by flow cytometry dot plots (Fig. 3.1.3B). Similarly, the hPSC cultured on 10% HSt-PMEDSAH-g dishes stored at 4^0C were also strongly positive for NANOG, OCT4, and SOX2 as shown by the immunofluorescence staining (Fig. 3.1.2.1B) and strongly co-expressing TRA 1-60/NANOG and TRA 1-81/NANOG as observed in flow cytometry dot plots (Fig. 3.1.3.1C). All these data was obtained using the chemically defined and xeno-free medium StemFlex. Comparable results were obtained using StemFit, mTeSR Plus and PluriSTEM-XF, all chemically defined and xeno-free culture media and immunostaining for NANOG, OCT4, SOX2 and SSEA4.

The pluripotency of hPSC cultured on the 10% HSt-PMEDSAH-g dishes was determined by embryoid body (EB) formation assay after 20 passages. Analysis of the EB indicated the expression of representative genes of the endoderm, mesoderm and ectoderm lineages. Quantitative analysis of self-renewal and pluripotency was assessed by the trilineage differentiation potential of hPSC cultured on 10% HSt-PMEDSAH-g dishes using TaqMan hPSC Scorecard Assay based on real-time qPCR assays (Fig. 3.1.3C). All of these findings demonstrated that 10% HSt-PMEDSAH-g supported the self-renewal and pluripotency of hPSC. We validated quantitatively the confirmed pluripotency (trilineage differentiation potential) of the cells cultured on the 10% HSt-

PMEDSAH-g dishes using real-time qPCR assays for several genes representing three germ lineages.

Since chromosomal changes may occur during long-term culture of hPSC, the genetic stability of cells cultured on 10% HSt-PMEDSAH-g dishes was evaluated by standard G-band analysis after 20 passages. The results demonstrated a normal human male karyotype for the H1 cell line (Fig. 3.1.3D).

3.1.4: Reprogramming of Human Somatic Cells on 10% HSt-PMEDSAH-g Dishes

Reprogramming of patient derived cells in chemically defined and xeno-free conditions will enhance the successful use of these cells in translational medicine to treat patient debilitating diseases. Thus, we investigated whether 10% HSt-PMEDSAH-g could have a positive impact on reprograming of fibroblasts into hiPSC (Fig. 4A). Sendai viral vectors carrying the *KMOS* cocktail were used to infect human gingival fibroblasts in both control (Matrigel coated dishes) and experimental groups (10% HSt-PMEDSAH-g dishes). On day 28, hiPSC colonies were classified as successfully reprogrammed, or as pre-iPSC by the following criteria: reprogrammed colonies should have positive AP staining, well-defined borders and cells should have a high nucleus: cytoplasm ratio (Fig 3.1.4A, Fig. 3.1.4.1A and B). We characterize the hiPSC developed on 10% HSt-PMEDSAH-g dishes as self-renewal and pluripotent. The hiPSC were strong positive for NANOG, OCT4and SOX2 as revealed by our immunostaining (Fig. 3.1.4B) and were more that 99% positive for SSEA3, SSEA4, TRA 1-60 and TRA 1-81 as shown by flow cytometry histograms (Fig. 3.1.4C). Similarly, the pluripotency of hiPSC obtained on 10% HSt-PMEDSAH-g dishes was determined by EB formation and we confirmed their tri-lineage differentiation potential using real-time qPCR assays for several genes

representing all germ lineages (Fig. 3.1.4D). As expected, the hiPSC developed on control group (Matrigel) were also self-renewing and pluripotent (Fig 3.1.4A, Fig. 3.1.4.1A and B).

We quantified the hiPSC colonies developed on Matrigel and 10% HSt-PMEDSAH-g dishes by staining for alkaline phosphatase and manually counting the colonies (Fig. 5A and B). Interestingly, the reprogramming efficiency was significantly higher ($p<0.0068$) in the 10% HSt-PMEDSAH-g dishes compared to the Matrigel group, 0.37% vs. 0.22%, respectively (Fig. 3.1.4.1C).

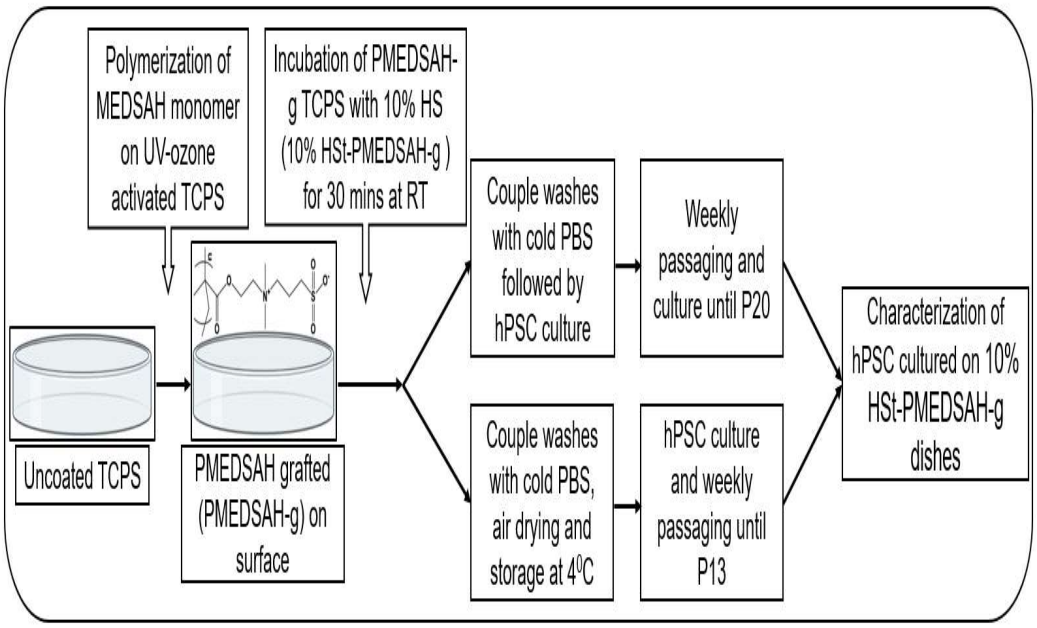

Figure 3.1: Schematic representation of the experimental protocol

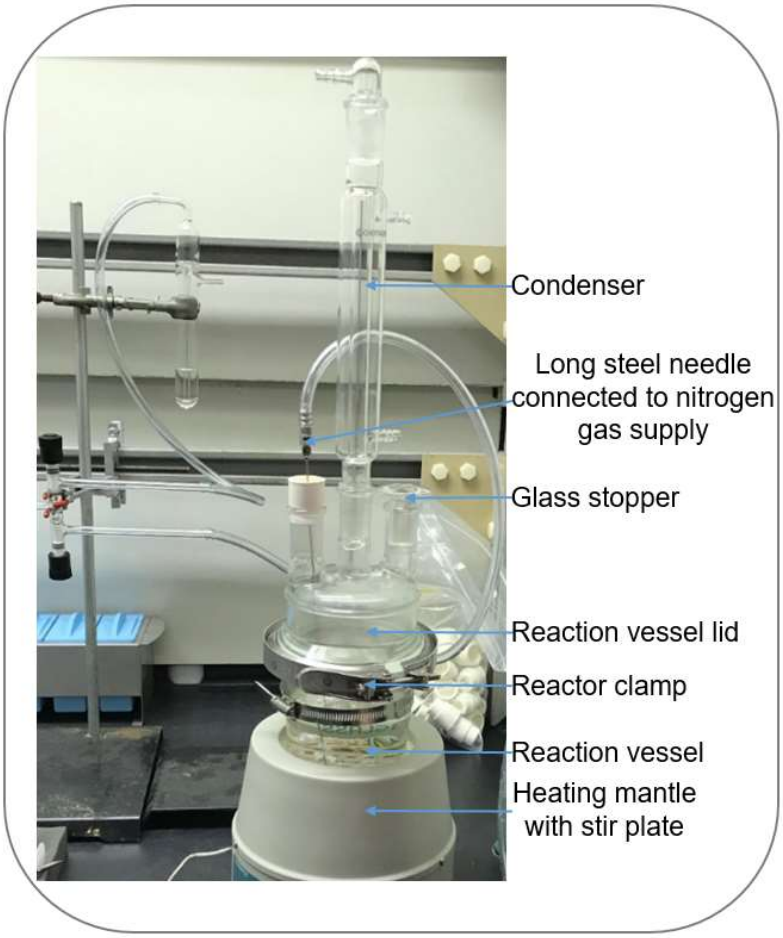

Figure 3.1.1: Reactor and set up to synthesize PMEDSAH grafted (PMEDSAH-g) dishes

Table 3.1: List of supplements/chemicals systematically tested along with chemically defined commercial media to promote the attachment and long-term maintenance and growth of hPSC on PMEDSAH-g dishes

Supplements to promote attachment				Concentration	Observations
Integrin activation	Divalent cations	Cytokines	Serum		
Commercial peptide (QHREDGS)				10nM	No cell attachment
Integrin activating antibody				2ug/ml	Low and unstable cell attachment on W0
Altering the pH of media used				7.0, 7.2, 7.4, 7.6, 7.8, and 8.0	Low cell attachment, which was lost by W1
	Ca^{2+}, Mg^{2+}, Mn^{2+}			3mM	Cell attachment sustained until W3
		Phorbol myristate acetate (PMA)		100ng/ml	No cell attachments
		Retinoic acid (RA)		1mM	Low and unstable cell attachment on W0
			Fetal Bovine serum (FBS)	10%	Cell attachments and differentiation
			Knockout™ Serum Replacement (KOSR)	10%	No cell attachments
			Human serum (HS)	1%	Low cell attachment on W0, lost all cells by W4
			HS	10%	Consistently stable, and long term cell attachment
			HS	100%	Highest cell attachment, but high degree of differentiation during each passage

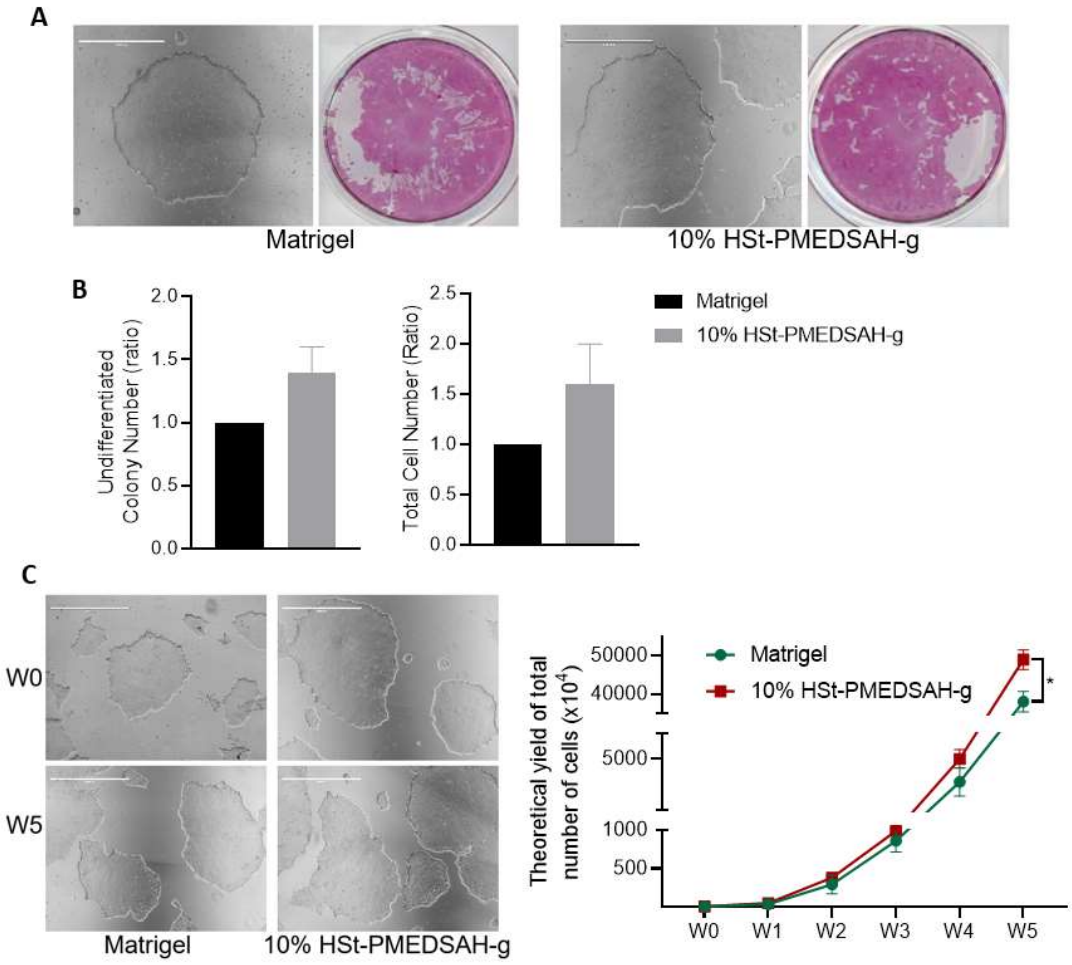

Figure 3.1.2: Culture and expansion of hPSC on 10% HSt-PMEDSAH-g dishes. PMEDSAH-g dishes treated with 10% HS (10% HSt-PMEDSAH-g) in DMEM/F12 gave better results for promoting and stabilizing cell attachment and long term culture of undifferentiated hPSC compared to cells cultured on Matrigel-coated dishes. Representative micrographs of hPSC colonies cultured on (A) Matrigel-coated plates and (B) 10% HSt-PMEDSAH-g. On the right side, respective alkaline phosphatase (AP) stained colonies. (C) Plot of undifferentiated colony number (ratio) and total cell number (ratio) compared to control group (Matrigel coated dishes) indicating that 10% HSt-PMEDSAH-g lead to a higher number of undifferentiated colonies and total number of cells on week 1. (D) Representative micrographs of hPSC colonies cultured on 10% HSt-PMEDSAH-g and Matrigel-coated plates during week 0 and week 5. The graph to the right indicate the theoretical yield of total number of cells counted and compared from colonies cultured on 10% HSt-PMEDSAH-g and Matrigel coated dishes during weekly passaging until passage 5. Scale bars, 1000 µm.

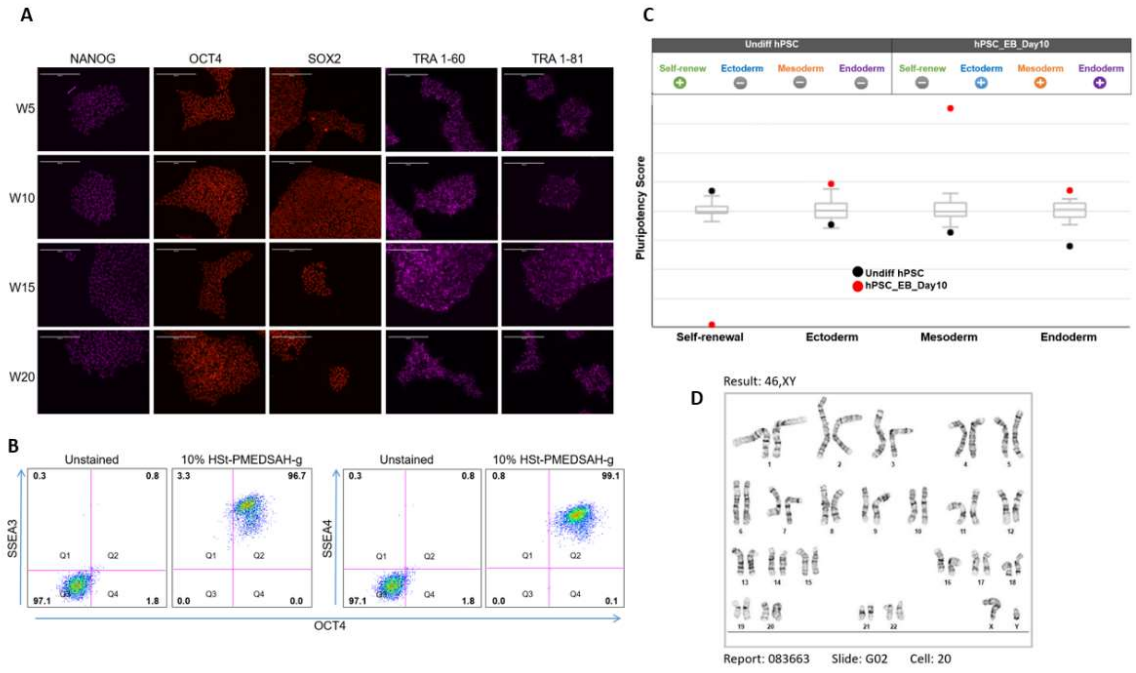

Figure 3.1.3: Characterization of hPSC after long-term culture on 10% HSt-PMEDSAH-g dishes. HPSC cultured on freshly prepared 10% HSt-PMEDSAH-g plates for 20 consecutive passages, maintaining self-renewal and pluripotency. Representative (A) micrographs of immunocytochemistry every 5 weeks showing strong positive reaction for human pluripotency markers, and (B) dot plots of hPSC after 20 passages of culture on freshly prepared 10% HSt-PMEDSAH-g dishes, showing more than 99% co-expression between SSEA3/OCT4and SSEA4/OCT4. (C) Pluripotency was confirmed by qPCR hPSC ScoreCard assay quantifying the self-renewal and trilineage differentiation potential of passage 20 hPSC cultured on 10% HSt-PMEDSAH-g and 10 days old EB's developed from same pool of cells. (D) G-banding karyogram of cells cultured on 10% HSt-PMEDSAH-g dishes at passage 20 confirming genetic integrity. Scale bars, 200 µm.

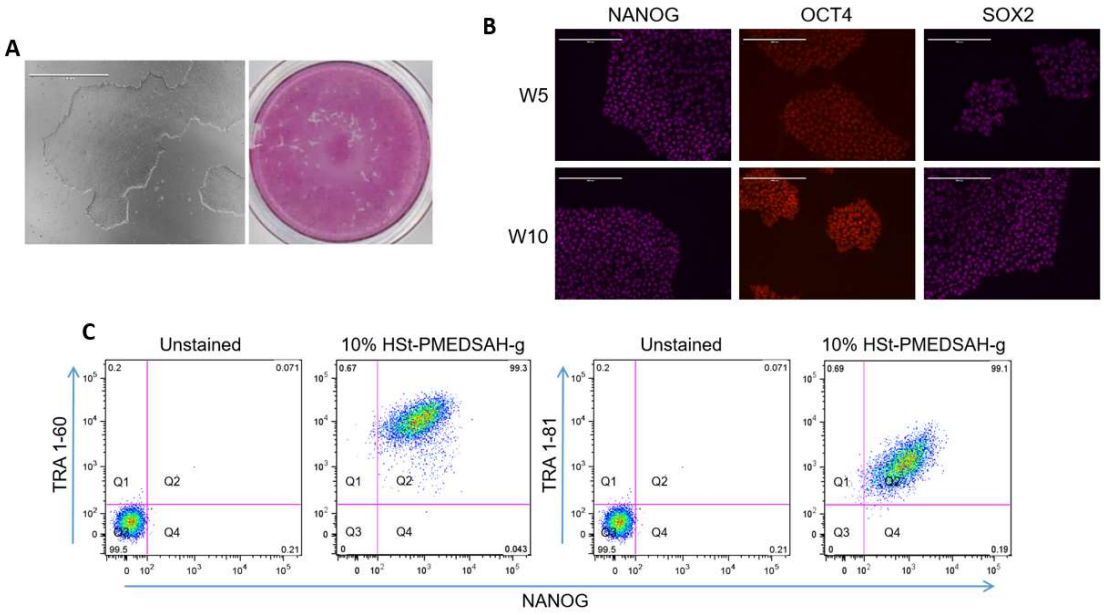

Figure 3.1.3.1: Characterization of hPSC cultured on 10% HSt-PMEDSAH-g dishes prepared and stored at 4^0C until use for weakly passaging. (A) Representative micrographs of hPSC colonies in bright-field and alkaline phosphatase staining after one week of culture on 10% HSt-PMEDSAH-g dishes. Scale bars, 1000 µm (B) Representative fluorescent micrographs of hPSC colonies stained with pluripotency associated markers (NANOG, OCT4and SOX2) after 5 and 10 consecutive passages (W5 and W10, respectively) of culture on 10% HSt-PMEDSAH-g dishes. Scale bars, 200 µm (C) Representative histograms of hPSC after 10 passages of culture on 10% HSt-PMEDSAH-g dishes, showing around 99% co-expression between TRA 1-60/NANOG and TRA 1-81/NANOG.

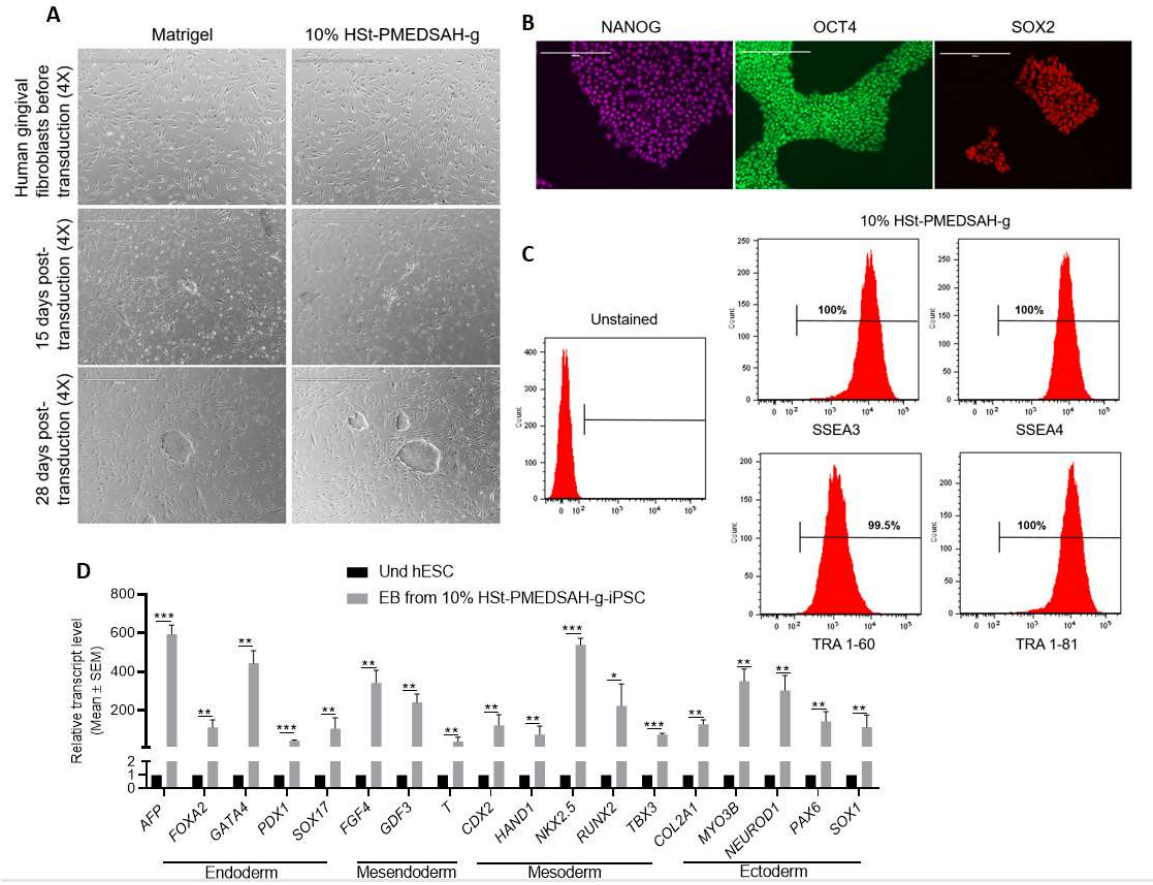

Figure 3.1.4: Reprogramming of human gingival fibroblasts into induced PSC (iPSC) on 10% HSt-PMEDSAH-g dishes. Human gingival fibroblasts were reprogramed into iPSC on Matrigel-coated dishes and on 10% HSt-PMEDSAH-g dishes. (A) Representative transmitted light micrographs showing the morphology of fibroblast before and during the development hiPSC colonies, Scale bars, 1000 µm. (B) Representative micrographs of hiPSC developed on 10% HSt-PMEDSAH-g plates after immunocytochemistry staining with pluripotency associated markers, Scale bars, 200 µm. (C) Representative histograms of hiPSC developed on 10% HSt-PMEDSAH-g dishes showing the expression of cell surface-pluripotency associated markers. (D) qPCR analysis for the expression of markers corresponding to all germ lineages showing trilineage differentiation potentiality of 10 days old EB obtained from hiPSC developed on 10% HSt-PMEDSAH-g dishes and compared to undifferentiated hESC. Scale bars, 200 µm.

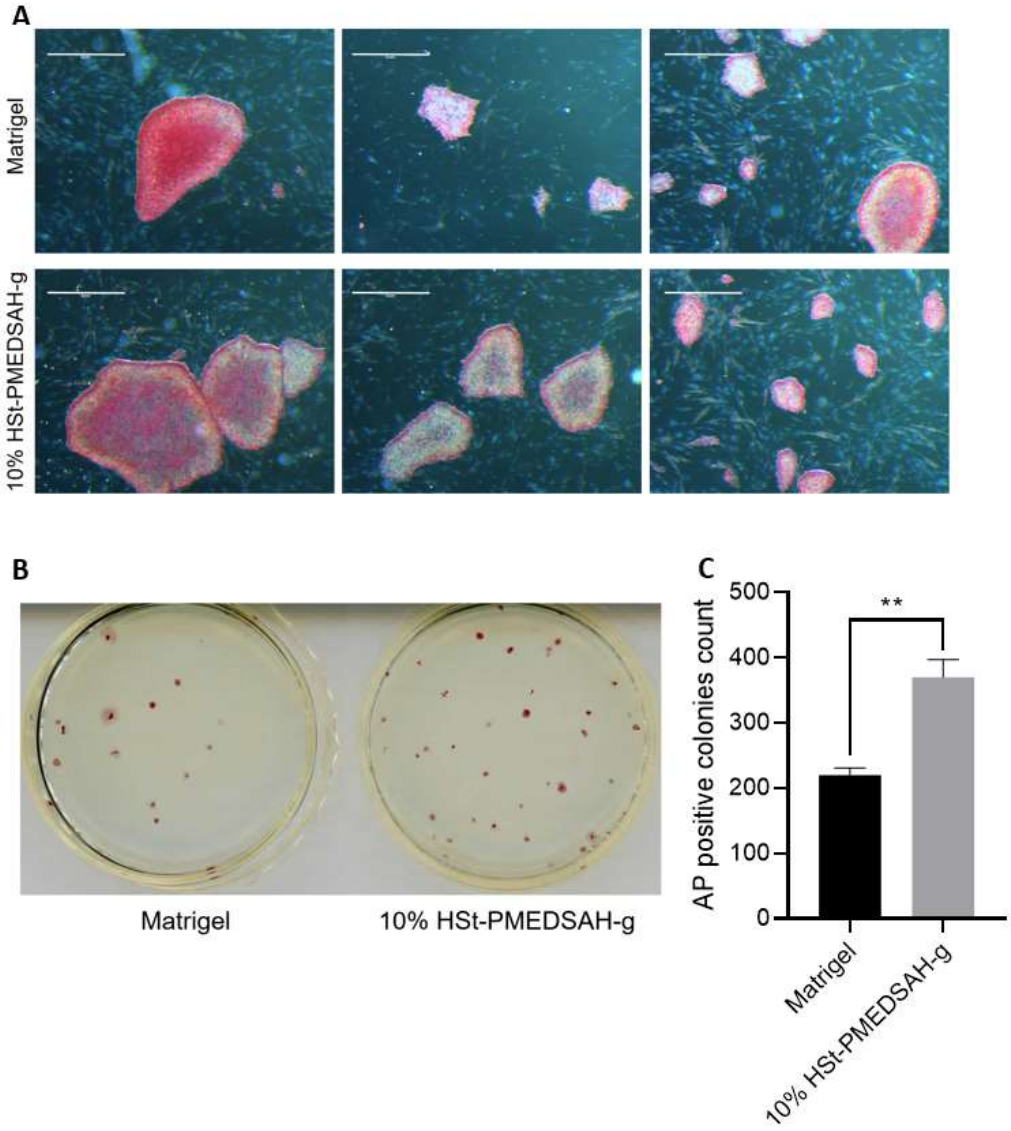

Figure 3.1.4.1: Reprogramming efficiency of human gingival fibroblasts into hiPSC in 10% HSt-PMEDSAH-g dishes. Human gingival fibroblasts were reprogrammed into iPSC on 10% HSt-PMEDSAH-g plates and Matrigel-coated plates. (A) Representative bright field images of iPSC colonies derived on 10% HSt-PMEDSAH-g and Matrigel coated dishes after staining for alkaline phosphatase (AP), Scale bars, 5mm. (B) Representative images of total colonies in each condition and (C) graph indicating the average (N=3) AP-positive colonies in each condition.

3.2: Simulated Microgravity (Sμg) and Study of Its Biological Role in Human Pluripotent Stem Cells (HPSC) Behavior

3.2.1: Simulated Microgravity Enhanced the Self-Renewal and Proliferation of hPSC

The effects of sμg on hPSC were investigated by comparing to cells cultured in normal gravity (1g). First, we examined and confirmed that hPSC cultured under sμg for 96 hours remained undifferentiated (Fig. 3.2.1.1A). The expression levels of pluripotent transcription factors (TFs) including the homeodomain protein NANOG, the POU domain transcription factor OCT4(also known as POU5F1), and the SRY-related HMG-box transcription factor SOX2 - required to establish the undifferentiated state and to maintain self-renewal of PSC (102-104), and the transmembrane glycoproteins integrin α6 (ITGA6) (also known as CD49f) and integrin β1 (ITGB1) (5, 49, 61), were analyzed at protein and RNA levels in cells under sμg and 1g conditions. Analysis of micrographs from colonies under both conditions indicated an increase in the immunofluorescent signal of NANOG, OCT4and SOX2 under sμg (Fig. 3.2.1.1A). These results were confirmed by quantification of protein bands obtained by immunoblotting (Fig. 3.2.1.1B). An increase in protein expression of ITGA6 was also observed, while no change was detected for ITGB1. Analysis at the RNA level indicated that *SOX2* was upregulated ~2-fold in cells under sμg in relation to 1g, while no difference was observed for the other pluripotent genes (Fig. 3.2.1.1C). It is known that the telomerase pathway is active and required for prolonged self-renewal in hPSC (97, 105), thus, we analyzed the expression levels of *TERT* and *ZCAN4*, genes involved in telomere elongation. The results demonstrated a significant increase in their RNA expression levels in cells under sμg compared to control ones (Fig. 3.2.1.1D). The higher RNA levels observed during sμg

returned to basal levels once the cells were further cultured in 1g (Supplementary Fig. 2). These results indicate that sμg sustains and suggest an enhancement in the self-renewal of hPSC.

We and others have identified a specific transmembrane protein "CD49f" that regulates self-renewal of stem cells and previous reports indicate that self-renewal of stem cells is enhanced in microgravity conditions. Here, we aim to investigate the expression and function of CD49f in stem cells cultured under simulated microgravity condition compared to normal gravity conditions. Our working hypothesis is that sμg enhances the expression of CD49f, leading to inhibition of cell differentiation, and thus maintaining, if not enhancing, the self-renewal of hPSC. Simulated microgravity reduces the susceptibility towards differentiation

We analyzed the differentiation capability of hPSC after culturing in sμg by inducing the formation of EB and found that the cells remained pluripotent, as indicated by increased transcript level expression of genes representative from all 3 germ layers. Due to the increased protein translation of pluripotent associated proteins in cells cultured in sμg compared to cells at 1g (Fig. 3.2.1.1A-C), we further tested whether their differentiation would be affected under sμg conditions. To do this, cells were first cultured in sμg with self-renewal- supporting medium for 48 hours, followed by 96 hours of further culturing using CDM with either BMP4 or RA to induce trophectoderm (106) and neuro-ectoderm (107) differentiation, respectively (Fig. 3.2.1.2A and B). As expected, the mRNA transcript levels for the core pluripotency transcription factors (*OCT4, SOX2*, and *NANOG*) were down-regulated after differentiation. However, the reduction was higher in cells cultured at 1g compared to cells at sμg. Genes related to

trophectoderm and neuro-ectoderm showed significantly higher increases in mRNA levels in cells cultured in 1g compared to sμg (Fig. 3.2.1.2A and B). These results support our previous observation that sμg conditions enhance the self-renewal of hPSC, as their differentiation is slightly delayed or reduced compared to 1g conditions.

We observed that under sμg the colony size and total number of cells counted per ug chamber were significantly higher as compared to 1g culture condition (Fig. 3.2.1.3 A-C). The enhanced cell proliferation of hPSC under sμg condition was supported by increased RNA levels of the cell proliferation marker, *KI67* (Fig. 3.2.1.3D). We analyzed the expression of 44 human cell cycle associated genes using a human cell cycle regulation gene array, which revealed that multiple genes change their expression after exposure to sμg (Fig. 3.2.1.3E). *CDK2/4* and their cyclin counterparts, *Cyclin E* and *Cyclin D*, respectively, along with the CDK activator *CDC25A* were significantly upregulated in hPSC cultured under sμg compared to 1g condition, whereas negative regulators were repressed in hPSC cultured under sμg condition (Fig. 3.2.1.3E). These results were validated by qRT-PCR analysis, which confirmed that *CDK2/4* and respective counterparts were significantly upregulated in hPSC cultured under sμg condition compared to 1g culture condition (Fig. 3.2.1.3F). The upregulated levels of cell cycle associated genes returned to levels comparable to cells under 1g condition after these cells were further cultured in 1g condition. To investigate whether the effects of sμg observed in hPSC would be replicated in somatic cells we cultured equal numbers of hFF in sμg and 1g conditions for 96 hours. The cell proliferation was not affected by sμg, as indicated by similar cell doubling time, and there were no differences in expression of *KI67* between hFF cultured in sμg and 1 g conditions. Similarly, the expression of

telomerase related genes in HFF was not affected by sμg, indicating a cell type dependent effect of sμg.

3.2.2: Simulated Microgravity Enhanced Self-Renewal by Modulation Proteasomal Complex Response

RNA sequencing analysis of hPSC cultured in sμg and 1g conditions identified 1741 differentially expressed (DE) genes (FDR <0.05) detected by the first four versions of the results. After intersection of these 1741 DE genes with the ones detected by Salmon analysis without alignment, 1649 genes DF were found by all five versions of gene expression results. From this common set of 1649 DE genes, 626 were over-expressed and 1023 were under-expressed in the sμg group compared to the 1g group. An unbiased gene set enrichment analysis using all available reactome pathways indicated that 532 and 677 pathways were upregulated in the sμg and 1g groups, respectively. Consistently with our results (Fig. 3.2.1.1 and 3.2.1.3), it was observed that pathways related to telomere maintenance and cell cycle were significantly upregulated in the sμg group compared to the 1g group, while in the 1g group pathways related to differentiation and development were up-regulated. Accordingly, among the top 20 differentially expressed genes between sμg and the 1g group were genes related to development and differentiation, such as *CYP26A1, HAS2, CRABP2, MEIS2, ID4, GRHL3* and *TUNAR*, which were down-regulated in the sμg group (Fig. 3.2.2.1). The analysis also showed that in 98 of the 532 up-regulated pathways in the sμg group the ubiquitin proteasome system was present. In particular, *PSMA1, 3* and *7*, and *PSMB5* from the core-20S particle, all six components of the base-19S regulatory particle (*PSMC1-6*), as well as *PSMD11* and *PSMD14* from the lid-19S regulatory particle were up-regulated. Real-time PCR analysis

validated the up-regulation of *PSMD11* in the sμg group compared to 1g condition (Fig. 3.2.2.2A), while an increase in PSMD11 protein translation in the sμg group was verified by ICC and WB analysis (Fig. 3.2.2.2B and C).

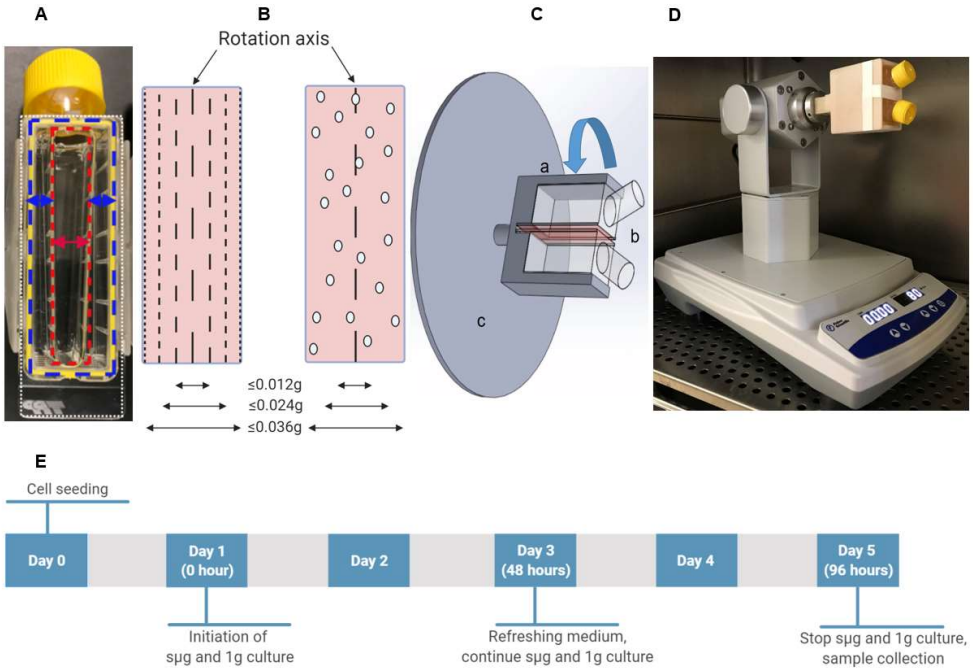

Figure 3.2: Experimental set up to simulate microgravity (sμg). A, Clipmax chamber-slides flasks with small culture channel created (represented by a red double sided arrow) after coating the two sides (represented by two blue double sided arrows) and the top of the chamber-slide flask (not shown) with PDMS. B, Distribution of microgravity forces in relation to the rotation axis at the slides where cells will be grown. Cells inside of the diameter area of 6, 12 and 188 mm in relation to the rotation axis will experience ≤0.012 g, ≤0.024 g and ≤0.036 g. Oval circles represent cells. C, Illustration of our developed device to sμg. (a) 3D printed adapter connects two cell culture flasks (b) to the spinning bolt of sample rotator (c). The bottom surfaces of the flasks where cells are attached (illustrated in red) are positioned back-to-back and located in the axis of rotation. D, Our developed rotary cell culture system (RCCS) with 2 flasks affixed to the system and located inside of cell culture incubator, ready generate simulated microgravity. E, Experimental design used in this project.

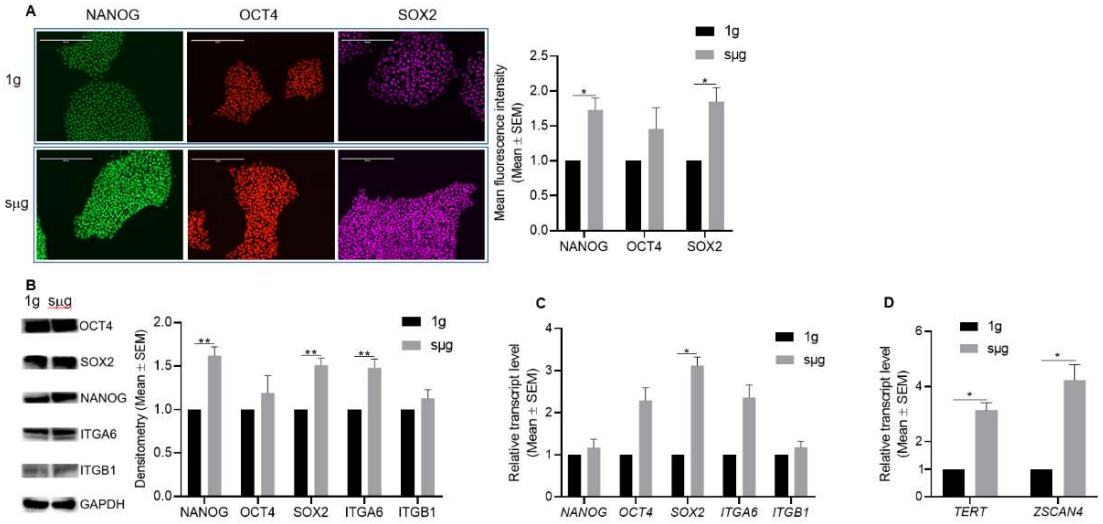

Fig. 3.2.1.1: Sμg enhances self-renewal of hPSC. Culture under sμg maintained self-renewal of hPSC and enhanced the expression of core set of pluripotency transcription factors, transmembrane glycoproteins ITGA6 and ITGB1, and telomere genes. A) Representative immunofluorescent micrographs of colonies from sμg and 1g conditions stained for core TFs. Graph shows the mean fluorescence intensity analysis from micrographs. Scale bars, 200 μm. B) Representative Immunoblots and C) densitometry analysis from protein lysates of cells cultured at 1g and sμg conditions. RT-qPCR analysis indicating relative mRNA levels of (C) pluripotent associated and (D) telomere elongation genes present in cells cultured at 1g and sμg. *P*-value calculated using unpaired *t*-test. Scale bars, 200 μm.

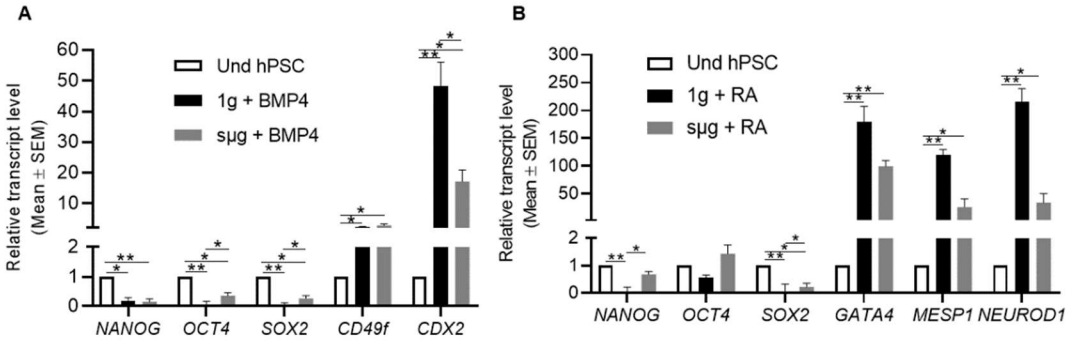

Fig. 3.2.1.2: Differentiation of hPSC is reduced under sµg conditions. hPSC were cultured under sµg or 1g for 48 h with medium that sustain their self-renewal, followed by further 48 h of cultured with differentiation medium to induced trophoectoderm (A) and neuro-ectoderm (B) differentiation. RT-qPCR analysis of representative genes related to pluripotency and trophectoderm and neuro-ectoderm indicated that differentiation under sµg conditions is reduced compared to 1g conditions. *P*-value calculated using unpaired *t*-test.

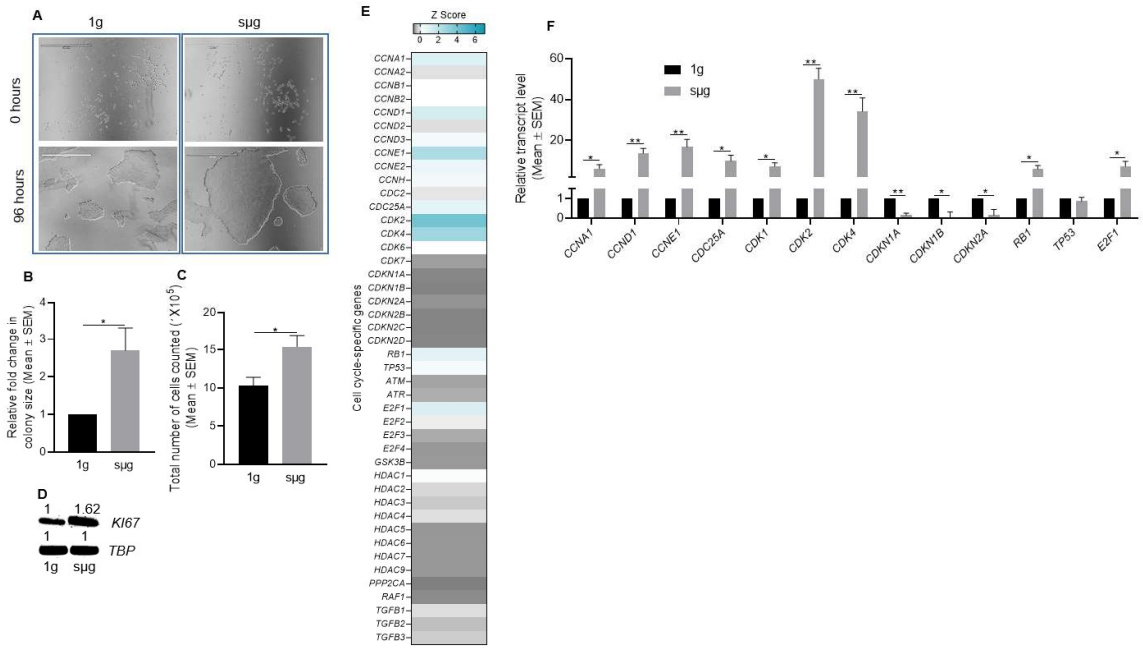

Fig. 3.2.1.3: Sμg enhances proliferation of hPSC. (A) Representative micrographs of hPSC colonies cultured under 1g and sμg conditions. (B) Graph indicating significant fold change difference in hPSC colonies area after 96 h of culture under 1g and sμg conditions. C) Graph comparing the total cell number of hPSC after 96 h of culture under 1g and sμg conditions. (D) Representative gel band images of rt-PCR analysis for the cell proliferation gene *Ki67* in hPSC after 96 h of culture under 1g and sμg conditions. The mRNA expression of *TBP* was used to show equal loading and to quantify the relative differences in expression, as indicated above each band. (E) Heat map showing the relative mRNA levels of 44 human cell cycle associated genes in hPSC culture under sμg for 96 h in relation to cells cultured in 1g condition. (F) RT-qPCR analysis was used to verify the expression of selected genes tested in the gene array assay. *P*-value calculated using unpaired *t*-test. Scale bars, 200 μm.

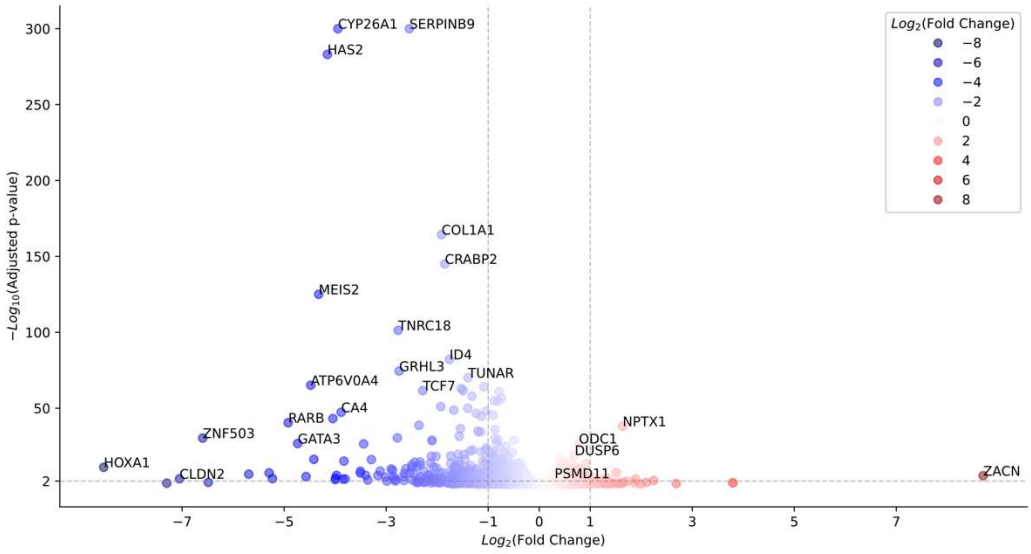

Fig. 3.2.2.1: Volcano plot of differential gene expression results. The color intensity is proportional to Log2 (Fold Change). Genes are overly expressed under sμg condition if Log2 (Fold Change) > 0 (colored red in the figure). The vertical dashed lines correspond to Log2 (Fold Change) =$\pm$1, and the horizontal line corresponds to adjusted p-value = 0.01. There are a few genes that are highly expressed under 1g condition such as HAS2, CYP26A1, SERPINB9, etc.

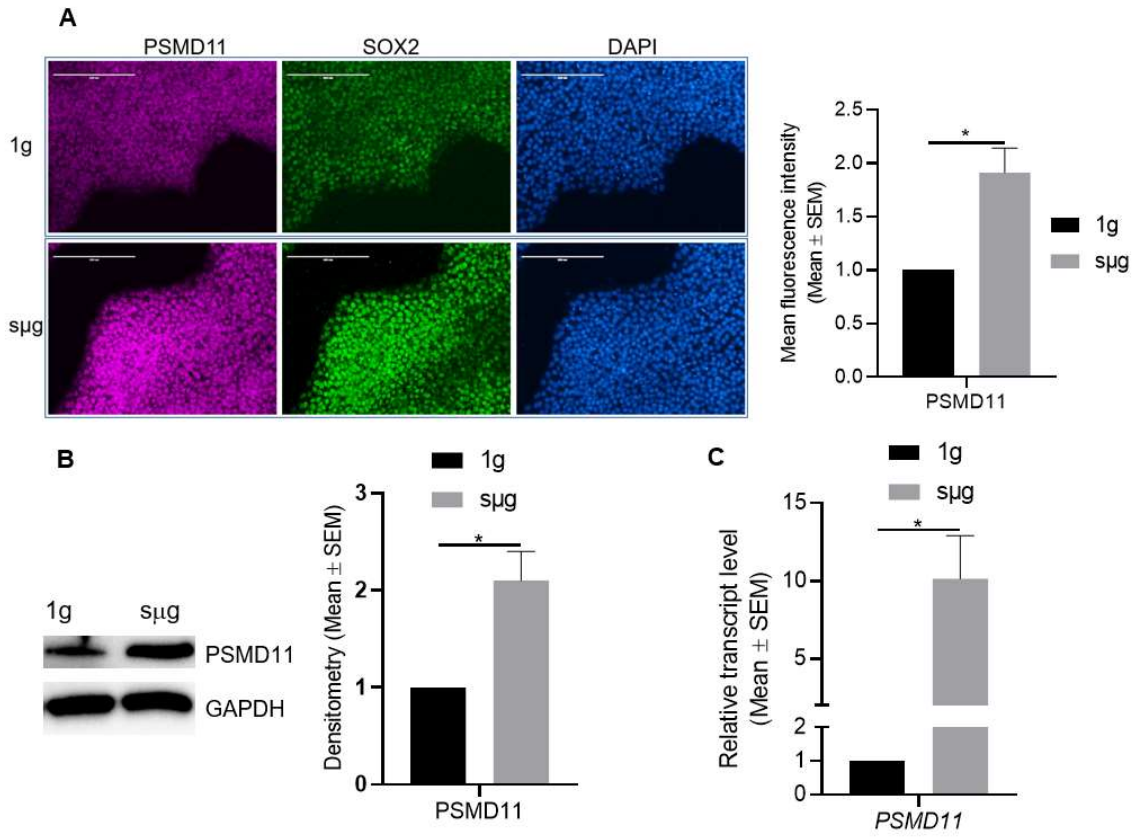

Fig. 3.2.2.2: Sμg enhances PSMD11 expression in hPSC. (A) Representative immunofluorescent micrographs of hPSC colonies cultured in sμg and 1g conditions and stained for PSMD11 and SOX2. DAPI was used to stain the nuclei of all cells. Scale bars, 200 μm. Graph showing the mean fluorescence intensity analysis from micrographs. (B) Representative Immunoblots and densitometry analysis of PSMD11 from protein lysates of cells cultured at 1G and sμg conditions. GAPDH was used as loading control. Graph on the right shows the densitometry analysis of the immunoblots. (C) RT-qPCR analysis indicating the relative mRNA levels of *PSMD11* present in cells cultured at 1g and sμg.

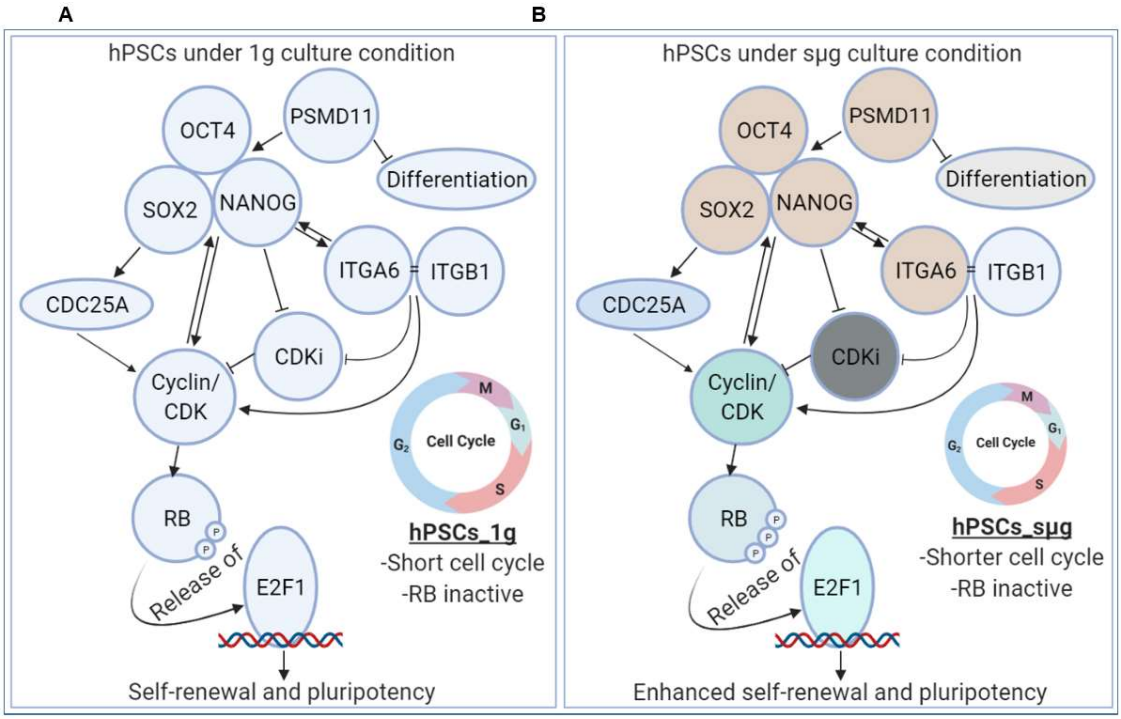

Figure 3.2.3: Schematic model of mechanisms behind the enhanced self-renewal and proliferation of hPSC cultured with sμg. (A) Under 1g conditions the interplay between the core set of pluripotent transcription factors (TFs: OCT4, SOX2, and NANOG), and the transmembrane glycoprotein heterodimeric complex formed by integrin a6 (ITGA6) and integrin b1 (ITGB1) maintain proliferation and self-renewal of hPSC by interacting with major regulators of the cell cycle. (B) The sμg model shows that hPSC's enhanced expression of PSMD11, sμggesting an increased ubiquitinase activity targeting differentiation related genes, while protecting the core pluripotent TFs (represented in brown color). This in turn upregulates (represented in green color) the expression of the major cell cycle regulators, while suppresses negative regulators of cell cycle progression (represented in grey color). Resulting in shorter cell cycle, enhance proliferation and maintaining prolonged self-renewal.

Table 3.2: List of probes used in RT-qPCR.

Gene Symbol	Assay ID
AFP	HS00173490_m1
ATM	Hs01112307_m1
ATR	Hs00354807_m1
CCNA1	Hs00171105_m1
CCNA2	Hs00153138_m1
CCNB1	Hs99999188_m1
CCNB2	Hs00270424_m1
CCND1	Hs00765553_m1
CCND2	Hs00153380_m1
CCND3	Hs00236949_m1
CDX2	Hs01078080_m1
CCNE1	Hs01026536_m1
CCNE2	Hs00372959_m1
CCNH	Hs00236923_m1
CDC2	Hs00364293_m1
CDC25A	Hs00947994_m1
CDK2	Hs01548894_m1
CDK4	Hs00175935_m1
CDK6	Hs01026372_m1
CDK7	Hs00361486_m1
CDKN1A	Hs00355782_m1
CDKN1B	Hs00153277_m1
CDKN2A	Hs00923894_m1
CDKN2B	Hs00365249_m1
CDKN2C	Hs00176227_m1
CDKN2D	Hs00176481_m1
E2F1	Hs00153451_m1
E2F2	Hs00231667_m1
E2F3	Hs00605457_m1
E2F4	Hs00608098_m1
FOXA2	Hs00232764_m1
GAPDH	Hs02786624_g1
GATA4	Hs00171403_m1
GSK3B	Hs00275656_m1
HDAC1	Hs02621185_s1
HDAC2	Hs00231032_m1
HDAC3	Hs00187320_m1
HDAC4	Hs00195814_m1
HDAC5	Hs00608366_m1
HDAC6	Hs00195869_m1

HDAC7	Hs00248789_m1
HDAC9	Hs00206843_m1
ITGA6	Hs01041911_m1
ITGB1	Hs00559595_m1
MESP1	Hs01001283_g1
NANOG	Hs02387400_g1
NEUROD1	Hs00159598_m1
PAX6	Hs00240871_m1
POU5F1	Hs04260367_g1
PPP2CA	Hs00427259_m1
RAF1	Hs00234119_m1
RB1	Hs01078066_m1
RUNX2	Hs01047973_m1
SOX2	Hs00602736_s1
T	Hs00610080_m1
TERT	Hs00972650_m1
TGFB1	Hs00998133_m1
TGFB2	Hs00234244_m1
TGFB3	Hs01086000_m1
TP53	Hs01034249_m1
ZSCAN4	Hs00537549_m1
PSMD11	Hs00160660_m1

3.3 Establishing CD49f as a Reliable Biomarker to Define Mesenchymal Stem Cells.

In addition to maintaining self-renewal of hESC, CD49f also sustains the self-renewal of somatic stem cells and cancer stem cells. We hypothesize that CD49f could be a reliable biomarker to define mesenchymal stem cells. Also, it has been shown that OCT4and SOX2 bind the promoters of CD49f, and we found that these transcription factors support CD49f expression during reprogramming into iPSC. Hence, we aim to characterize the transcriptional regulation of CD49f in mesenchymal stem cell types and this characterization will shed light in transcription factors regulating this stem cell type, which has the potential to be translated into designing of "reprogramming cocktails" for direct reprogramming of somatic cells into mesenchymal stem cells.

As expected, the derived MSC maintained a spindle morphology over eight passages; however, the capacity for adipocyte and osteoblast differentiation was significantly reduced from passage 3 to passage 6 and was almost non-existent by passage 8 (Fig. 3.3.1A). Calculations for cell doubling time indicated a significant decrease in proliferation rates between passage 3 and passages 6 and 8, which was validated by a 30% decrease in *KI67* RNA levels (Fig. 3.3.1B and C), indicating the differentiation and proliferation were reduced in MSC during *in vitro* propagation.

Flow cytometry analysis of MSC at passages 3, 6 and 8 demonstrated that CD105 and CD29 biomarkers remained highly expressed in MSC during all cell passages, while CD146 and CD271 were minimally expressed (Fig. 3.3.2A). CD49f and CD73 were highly expressed at passage 3, decreased significantly ($P < 0.05$) at passage 6 and returned to high levels at passage 8. CD45 expression was low at passage 3 and increased with subsequent subculture. The expression of all these biomarkers was comparable to

levels identified in foreskin and gingival fibroblasts with the exception of CD49f, which was low (<10%) in fibroblasts. Differences in expression of CD49f between fibroblasts and MSC were validated at RNA levels, with an 88.9 ± 37.9 (mean ± SEM) fold increase in MSC in relation to fibroblasts.

I further investigated the mRNA expression CD49f in MSC at passage 3 and in equivalent cells in early process of differentiation into osteoblasts and adipocytes. Results indicate decreased expression of CD49f in cells undergoing adipogenic and osteogenic differentiation (Fig. 3.3.2B).

Finally, the magnetic beads sorted early passage MSC for CD49f positive and negative cells using specific FITC conjugated monoclonal antibody targeting CD49f showed that the multipotency and self-renewal capabilities of CD49f negative MSC were significantly low in comparison to CD49f positive MSC (Fig. 3.3.3A-F), suggesting that CD49f can be used to identify functional MSC population. Hence, the results identify CD49f as a reliable biomarker that better indicate the functional status of MSC.

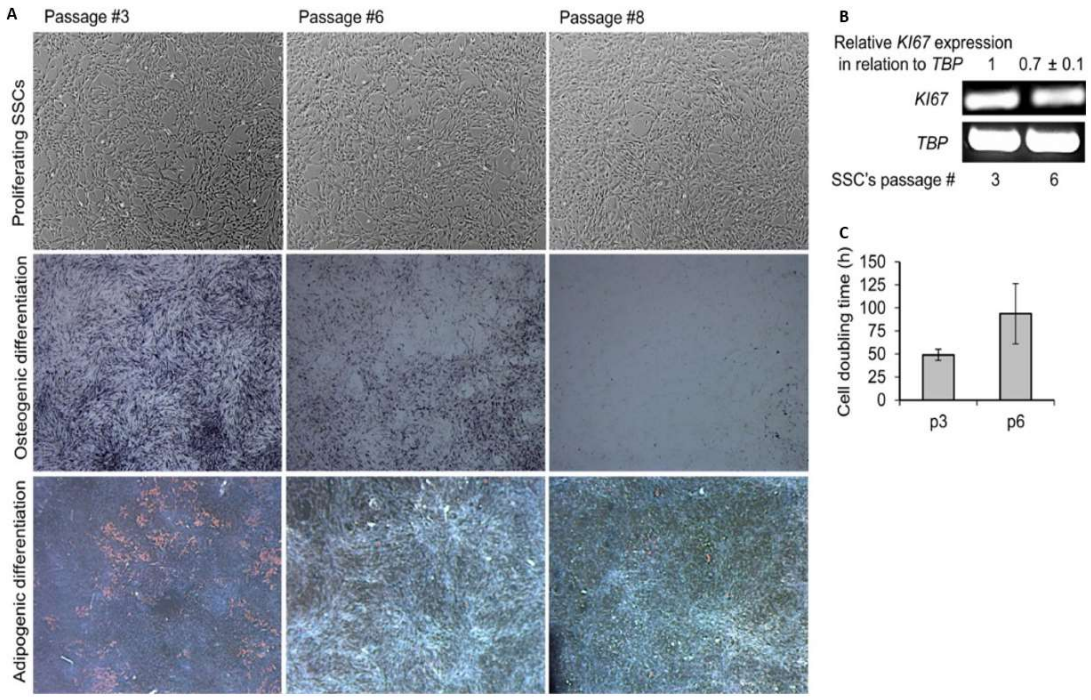

Figure 3.3.1: MSC lost potential for differentiation and proliferation over time. hPSC-MSC were derived and sub-cultured for eight consecutive passages. **a** Top panel shows representative micrographs of MSC at passages 3, 6 and 8 to highlight that the cell spindle morphology of these cells remains through all passages. The middle panel and bottom panel show representative micrographs of osteoblasts and adipocytes from MSC of respective passages and after staining for alkaline phosphatase and Oil Red O, respectively. **b** Representative image of RT-PCR gel showing reduction in KI 67 expression in MSC at passage 6 compared to cells at passage 3. **c** Graph indicating cell doubling time in hours (h) of MSC at passages 3 and 6. At early passages, the cells were functionally active - indicated by active proliferation and differentiation capability, whereas these characteristics declined drastically during late passages.

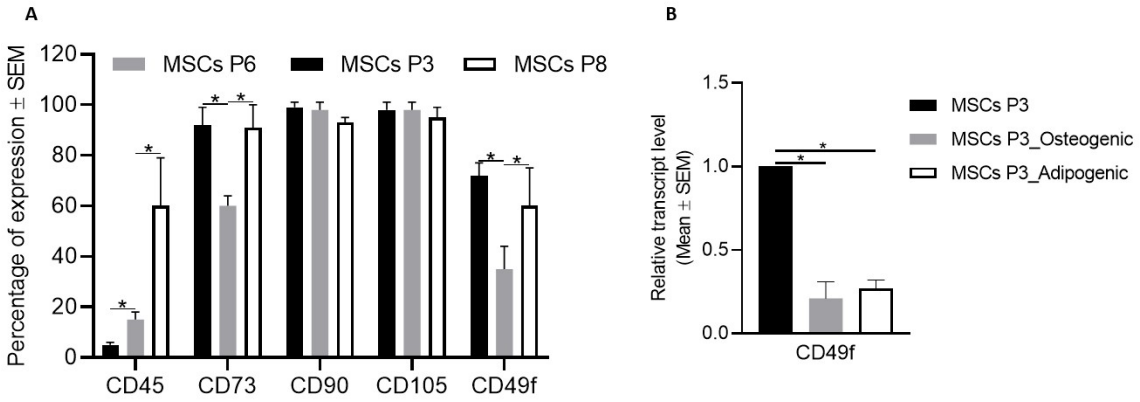

Figure 3.3.2: Expression of cell surface biomarkers in MSC**. a** Flow cytometry analysis was performed on MSC at passages 3, 6 and 8 to quantify the percentage of cells with positive expression of different biomarkers. The expression of commonly used positive selection biomarkers remained highly expressed from early to late passages MSC, whereas the expression of CD49f remained high until passage 3 and declined in subsequent passages. **b** RT-qPCR analysis showing relative mRNA expression of CD49f on early passage MSC, and same cells after differentiation to osteogenic and adipogenic cells showing decreased expression in cells undergoing differentiation.

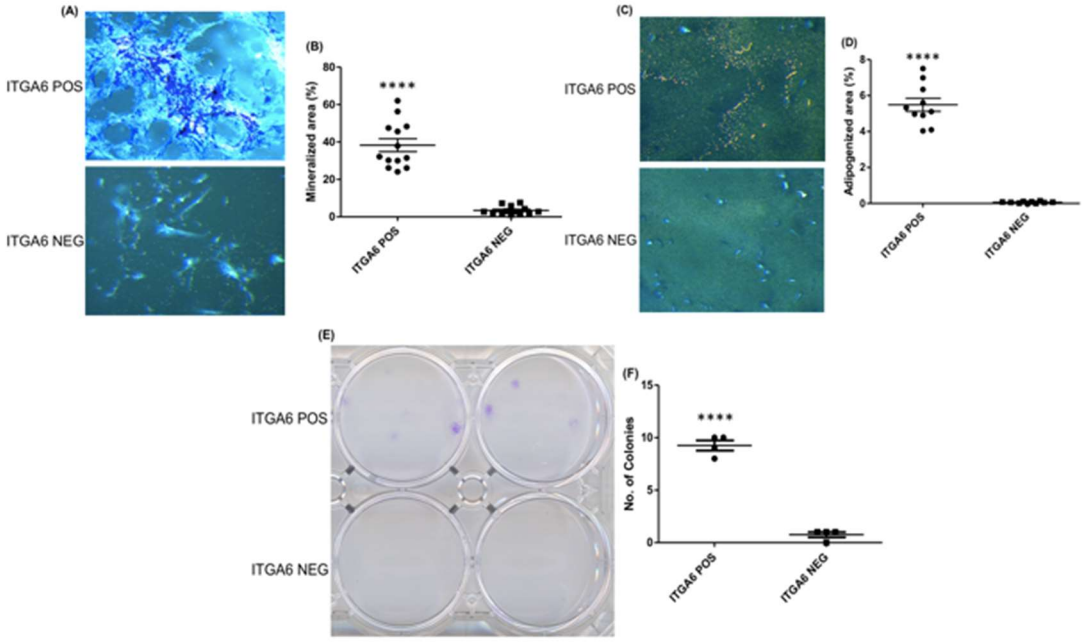

Figure 3.3.3: Enhanced stemness, and multipotency properties of CD49f positive early passage MSC. hESC-MSC at passage 3 were sorted out to separate CD49F positive and negative cells using specific monoclonal antibody targeting CD49F. Thus, sorted cells were sub-cultured and started the protocol for osteogenic and adipogenic differentiation and CFU assay. Once the respective protocols for osteogenic, adipogenic and CFU assay were over the cells were stained for alkaline phosphatase, Oil red O and with crystal violet, respectively. **a** Representative micrographs for osteogenic differentiation of MSC of respective groups. **b** Quantitation of mineralized area in respective groups. **c** Representative micrographs for adipogenic differentiation of MSC of respective groups. **d** Quantitation of area with lipid droplets in respective groups. **e** Representative micrographs for CFUs counted for respective groups. **f** Quantitation of CFUs in respective groups A significantly low osteogenic and adipogenic differentiation and self-renewal capability was observed in CD49F (CD49f) negative MSC in comparison to positive MSC, suggesting that CD49F can be used to identify functional SSC populations.

CHAPTER FOUR

CHRONOLOGICAL RELEVANCE AND DISCUSSION

4.1: Chronological Relevance

To utilize hESC in industrialized regenerative medicine and drug development, the culture methods must be improved to meet the technological standards in safety, cost-effectiveness, and the easiness of handling. Many of the common culture conditions are based on undefined support systems and contain the xenogeneic components limiting the ability to use pluripotent stem cells to treat debilitating human diseases. To overcome these problems, large efforts have been made to formulate defined and xenogeneic-free culture media and extracellular matrices. In these culture media, the most common cytokine is bFGF, which activates MAPK and/or PI3K-AKT signaling pathways. The second is Nodal/Activin/TGFβ, which activate TGFβ-SMAD signaling pathway. Activation of these signaling pathways is critical to maintain hPSC self-renewal (108).

Moreover, as hPSC are anchorage-dependent cells they require specific ECM and other proteins, peptides, or synthetic polymers as culture substrates to maintain their self-renewal. Other than natural or recombinant proteins, some synthetic materials have been developed to maintain hPSC self-renewal and which have a synthetic surface composed of RGD (Arg-Gly-Asp) containing short peptides covalently immobilized on acrylate coating to mimic the natural cell environment (109). Our team reported the first fully defined synthetic polymer coating, which maintained long-term growth of hESC in different culture media, and was poly[2-(methacryloyloxy)ethyl dimethyl-(3-sulfopropyl)ammonium hydroxide] (PMEDSAH) (110).

The importance of substrate on which pluripotent stem cells (PSC) are cultured to sustain self-renewal, and that the stem cells are able to sense and respond to biological, mechanical and topographical characteristics of the substrate has already been concluded(62, 110, 111). As the plasma membrane of the cells is in direct contact with the substrate, micro-environmental signals are first detected by protein receptors (majorly, family integrins (2)) at the plasma membrane and are transmitted towards the cell nuclei. In particular, we and other have identified CD49f, which is commonly expressed in all 35 identified stem cell types, as a key player in regulating self-renewal of pluripotent stem cells, skeletal muscle stem cells, glioblastoma, and breast cancer stem cells(61). All these strongly indicate key roles of CD49f in stem cells, which merit further investigation. More importantly, understanding the mechanisms that regulate the fate of PSC will advance their use in biomedical applications.

On the other hand, gravity is a physical force that affects the physiological functions of cells, tissue and organs. There are several studies indicating that self-renewal of stem cells is enhanced in microgravity conditions. However, there is not report on the effects of simulated microgravity (sμg) on hESC. Simulated microgravity is an ideal experimental condition to investigate self-renewal mechanisms of stem cells. It has been observed that during spaceflight diverse physiological conditions are affected, including loss of muscle mass, compromised immune system, susceptibility to ocular cataracts, loss of bone density, cardiac stress, among others, indicating that tissue regeneration is affected, and this might be due to altered stem cell behavior(112-114). Stem cell research has been performed at zero gravity during spaceflights or in sμg conditions (<1g, where g is the force of gravity) at earth, to understand the biological effects of microgravity on

human health (115-118). Interestingly, it has been observed that the capacity for differentiation is reduced in stem cells at microgravity, while their self-renewal is enhanced, this compared to cells cultured at earth gravity (1g) (115-118). In microgravity conditions, mesenchymal stem cells (MSC) show reduced capacity to differentiate into bone tissue, while mouse PSC retain their undifferentiated characteristics in culture conditions that normally induce differentiation. This indicates that studies at microgravity can shed light in potentially new molecular mechanisms involved in self-renewal of stem cells. Thus, here we propose studies using sμg to elucidate molecular mechanisms involved in self-renewal of hESC.

4.2: Optimization and Standardization of Culture Condition for hPSC

Owing to the intrinsic capability for unlimited self-renewal and the ability to make all the cells in the body, pluripotent stem cells (PSC) are an ideal candidate to be used as starting material for cell therapies. Much effort has been put into creating methods for human PSC (hPSC) expansion that are defined, robust, simple and safe. The evolution of hPSC culture from feeder-cell dependence and non-defined conditions to feeder-free and defined microenvironments has been enabled by the development of new culture materials (108). Thus, the development of a standard hPSC culture methods using completely defined and xeno-free culture environment that is able to support hPSC self-renewal, pluripotency and long-term propagation will advance our knowledge of PSC biology, and also increase the effectiveness of hPSC expansion on defined conditions for potential human applications. In this study, we established a chemically defined and xeno-free culture system for long-term culture and maintenance of hPSC while preserving their key molecular and functional features of hPSC. Furthermore, the culture

system described here also permitted the derivation of xeno-free hiPSC. In this regard, the culture of hPSC in chemically defined and xeno-free conditions will contribute substantially to future biotechnological and medical applications.

Our original protocol was based on culturing hPSC on PMEDSAH-grafted (PMEDSAH-g) TCPS dishes using human cell conditioned commercial medium (HCCM) (110). Herein, we report chemically defined and xeno-free culture of hPSC on PMEDSAH-g dishes pre-conditioned with 10% human serum (HS) in DMEM/F12 (10% HSt-PMEDSAH-g). We optimized the PMEDSAH grafting of the TCPS dishes and standardized their use for cultivation of hPSC. Our standardization of cultivation of hPSC on PMEDSAH-g dishes primarily focused on finding a reliable method for better adherence of hPSC and their long-term maintenance in xeno-free conditions. For this we did a systematic study by supplementing and treating (pre-conditioning) of PMEDSAH-g dishes. We found that pre-conditioning of PMEDSAH-g dishes with 10% HS in DMEM/F12 gave better and consistent result for attachment, and long-term culture and maintenance of hPSC.

In order to maintain hPSC pluripotency, a stem cell niche requires not only growth factor signals but also cell adhesion. Without the support of exogenous adhesion proteins, hPSC either die or differentiate (119, 120). Hence, hPSC are anchorage-dependent cells that utilize integrins for adhesion to substrates and it is also known that integrin signaling is important in hPSC cell adhesion, self-renewal and pluripotency maintenance (61, 121-124). Thus, we employed several methods to activate integrin signaling and tested the effect on cell adhesion and maintenance. It has been suggested and reported that angiopoietin-1 can directly support cell adhesion mediated by integrins

(87, 88, 125). Also, activation antibodies are thought to facilitate cell adhesion by converting low affinity integrin molecules to a high affinity state through direct binding and induction of conformational changes (89, 90, 126). In addition, several publications have reported that the attachment of mammalian cells to solid substrate is followed by an increase of intracellular pH and this pH shift is mediated by the Na+/H+ antiporter, which is obligatory for the development of the cell adhesion (91, 92, 127). Based on these findings, here, we tested the peptide motif (QHREDGS) derived from angiopoietin-1, the integrin binding site in angiopoietin-1 to promote cell adhesion (87, 88, 128). We also tested the compatibility of integrin activating antibody, and also tested the commercial media used in this project with varying pH with an aim to promote and stabilize cellular adhesion on the PMEDSAH-g dishes. However, we were not able to observe any improvement in cell attachment using these supplements.

Furthermore, several reports indicate that divalent cations, including Ca^{2+}, Mg^{2+}, Mn^{2+}, control not only cell-substrate adhesion but also laminin expression (93, 94, 129, 130). However, the supplementation of additional divalent cations to the media used to culture hPSC on the PMEDSAH-g dishes didn't support cell adhesion. Others have reported that cytokines regulate cell proliferation and cell adhesion to cell substrate (96, 127). We tested retinoic acid (RA) and phorbol myristate acetate (PMA) which were previously reported to enhance mammalian cells, including hPSC, adhesion to matrix, but similar to other supplements tested, our results indicated no support for cell attachment and proliferation of undifferentiated hPSC into the PMEDSAH-g dishes using a chemically defined and xeno-free media.

To keep cells alive for longer periods of time and to evaluate proliferation, migration and differentiation a basal medium must be supplemented with several factors. Serum derived from animals or humans is commonly used to maintain and proliferate cells. Fetal bovine serum (FBS) used in cell expansion protocols provides vital nutrients, attachment factors, toxin scavengers and growth factors, which are essential for the growth and maintenance of cells. We observed that supplementation of FBS to the hPSC culture media gave better attachment of cells on the PMEDSAH-g dishes, however also promoted certain degree of cell differentiation. In addition, it is also unsuitable for therapeutic purposes due to the ill-defined nature, high lot-to-lot variable composition, the risk of transmitting infectious agents and immunizing effects (98). Therefore, a continuous search for alternative sources for human cell cultivation that replaces the FBS in ongoing. Knockout™ Serum Replacement (KOSR), on the other hand, is for serum-free culture of PSC from multiple species. This defined, serum-free formulation directly replaces FBS in existing protocols as it alleviates many of the drawbacks of using FBS in stem cell culture, including differentiation of cells and heat-inactivation (120). However, during our investigation, KOSR failed in promoting cellular adhesion and growth of hPSC on PMEDSAH-g dishes. Recent studies have suggested that human body fluids including autologous serum, allogeneic human serum (HS) , and umbilical cord blood serum, platelet derivatives and follicular fluid could be promising substitutes (99, 131). Yet, there have been controversial issues about the advantages of HS, and detailed studies about the effects of HS on stem cells have not been done. Through our systematic study with gradient concentration of HS we reported that supplementation of hPSC culture media with 10% of HS gave better result with cell adhesion and growth compared to

FBS. Interestingly, pre-conditioning of freshly prepared PMEDSAH-g dishes with 10% HS in DMEM/F12 (10% HSt-PMEDSAH-g) under both the conditions -fresh use cell culture and stored at 4°C for weekly passaging-, supported better attachment, growth and long-term maintenance of hPSC. Furthermore, we successfully used several chemically defined and xeno-free commercial media to cultivate hPSC on 10% HSt-PMEDSAH-g dishes.

As Matrigel is the most commonly used feeder-free substrate for hPSC culture, it was used as a control in our experiments. A key concern in hPSC research is to maintain the pluripotent cultures in an undifferentiated and proliferative condition without causing chromosomal aberrations. We found that the 10% HSt-PMEDSAH-g led to higher number of undifferentiated colonies and total number of cells compared to the experimental group. In addition, the theoretical yield of total number of undifferentiated hPSC was observed to be significantly higher under 10% HSt-PMEDSAH-g culture condition compared to the control group. The hPSC cultured on freshly prepared 10% HSt-PMEDSAH-g dishes and also the 10% HSt-PMEDSAH-g dishes stored at 4^0C retained their self-renewal, pluripotency and a normal karyotype after multiple passages during culture, which indicates that hPSC maintained their unique characteristics and genomic stability. We showed this response of culture of hPSC on 10% HSt-PMEDSAH-g dishes using multiple chemically defined commercial media. These findings are well aligned with the long-term goal of large-scale production of clinical grade hPSC and hiPSC. In addition to significantly higher efficiency in hPSC expansion during long-term culture, the 10% HSt-PMEDSAH-g dishes have the following advantages compared to Matrigel: defined composition, long-term storage stability with minimal lot-to-lot

variability, easy preparation and compatibility with standard sterilization techniques. All of these features make the 10% HSt-PMEDSAH-g dishes a very promising substrate to obtain scalable populations of clinical grade hPSC. This could be accomplished by reducing the cell expansion time, production cost, as well as possible contamination and population drift under current culture conditions.

Induced pluripotent stem cells (iPSC) are obtained after genetic reprogramming of somatic cells (e.g., fibroblasts and blood cells) into a cell which acquires characteristics of PSC: self-renewal and capacity for differentiation in all cell types of the body (38, 102, 132). The human iPSC present a uniquely scalable platform for the study of inherited diseases, cell modeling, and as a novel mean for cell replacement in clinical applications; thereby, replacing the controversial use of hPSC. Despite having tremendous therapeutic potential, the translational research of hiPSC replacement therapy to human patients is relatively slow, highlighting the urgency for improved hiPSC-based cell therapy. Following the pioneering study by the Yamanaka group, others have used different strategies to produce hiPSC to meet the safety and quality criteria for effective therapeutic applications, in addition to increase the reprogramming efficiency. Since we observed significantly higher efficiency in hPSC expansion on 10% HSt-PMEDSAH-g dishes, we anticipated that the reprogramming efficiency into hiPSC will be enhanced under 10% HSt-PMEDSAH-g culture conditions. As we have previously reported (133), here we again used non-integrating Sendai virus constructs to overexpress OCT4, SOX2, KLF4, and C-MYC in human gingival fibroblasts and reprogrammed them into hiPSC under completely defined and xeno-free culture condition using our 10% HSt-PMEDSAH-g dishes. Remarkably, we observed that the reprogramming efficiency was

significantly increased when human somatic cells were reprogrammed into iPSC under 10% HSt-PMEDSAH-g culture condition compared to the Matrigel control group.

In summary, we have established a chemically defined and xeno-free culture condition for long-term maintenance and derivation of hPSC using our optimized and standardized 10% HSt-PMEDSAH-g dishes. The karyotype of hPSC remains stable after long-term culturing *in vitro*. Furthermore, the chemically defined and xeno-free culturing system also permits efficient derivation of hiPSC from human fibroblast through reprogramming. The xeno-free and chemically defined culture conditions described in this protocol are ideal for reducing lot-to-lot variation and increasing reproducibility, which can ensure consistency for the use of hPSC in both basic research and clinical applications. The long-term maintenance of hPSC without compromising safety and functionality in this defined culture system will reduce the economic burden for large-scale expansions for various applications. Our culture system has promising potentials for the wide applications of hPSC in *in vitro* studies to better understand developmental biology, and paves the way for translating hPSC and hiPSC technology to the clinic.

4.3: Self-Renewal of hPSC is Enhanced Under Sμg Culture Condition

To our knowledge, this is the first study that has investigated the self-renewal properties of hPSC in sμg, and demonstrated that the proliferation and self-renewal of adhered hPSC are enhanced under sμg compared to cells in 1g condition. This was accompanied by a modulated increase in protein expression of pluripotent TFs and integrin α6, as well as by up-regulation of telomerase activity and cell cycle associated genes. The RNA-seq analysis revealed that under sμg the expression of pathways related to differentiation and development were down-regulated, while multiple components of

the ubiquitin proteasome system were up-regulated, contributing to the enhanced self-renewal phenotype observed.

Multiple studies have shown that the capacity for differentiation of stem cells is reduced in ug conditions while their self-renewal is enhanced, suggesting that molecular mechanisms involved in self-renewal of stem cells are modified. Studies of mouse embryonic stem cells (mESC) under sμg have shown varied outcomes including decreased cell numbers associated with increased apoptosis, altered adhesion properties, and differentiation (134). It has been shown that spaceflight preserves the stemness of mESC-derived progenitors and inhibits the expression of markers of terminal differentiation for tissues derived from the three primary germ layers(115). Another study revealed that the need for a feeder layer, serum and Leukemia-Inhibitory Factor in the conventional method to prevent m ESC to spontaneously differentiate was eliminated by 3D clinostat culture (135). These studies are in agreement with our results using hPSC following 96 hours of cultivation under sμg and in adhering conditions, indicating that cells remain undifferentiated and that their self-renewal is enhanced compared to 1g culture conditions, as revealed by the increased protein levels of the core set of pluripotent TF. Blabber et al., 2015 (115) also reported that multiple markers indicative of self-renewal of stem cells were increased under sμg. We previously identified integrin α6 (also known as CD49f) as a key regulator in the self-renewal of hPSC and as the only commonly stem cell related protein expressed in all 35 identified stem cell types (5, 61). Here, we also observed that sμg upregulates the expression of integrin α6 in hPSC in comparison to the 1g control group. Further, our data indicates an induction of telomere elongation in hPSC cultured under sμg condition compared to 1g

culture condition, supported by the mRNA upregulation of *TERT* and *ZSCAN4*, which are known to contribute to telomere elongation (97, 105, 136). All of these findings indicate that sμg culture condition enhances the self-renewal of hPSC.

Our study demonstrated that hPSC cultured under sμg condition remained pluripotent after returning to 1g conditions, as shown by trilineage differentiation profiling of cells. However, the induced differentiation experiments towards trophectoderm and neuro-ectoderm during sμg showed that the reduction of pluripotent TFs was less evident in cells compared to 1g. The mRNA expression levels for trophectoderm and neuro-ectoderm markers were significantly lower in cells under sμg culture condition when compared to 1g. All of these suggest that sμg reduces susceptibility of hPSC towards differentiation, supporting our conclusion that sμg enhances their self-renewal.

PSC persist in a state of rapid proliferation and they have a unique short cell cycle, which in part serves to impede differentiation (137-140). We have shown that cell proliferation of hPSC is increased under sμg culture conditions. We found significantly larger colonies and high total number of cells under sμg compared to 1g culture condition and this was accompanied by significantly higher expression levels of *Ki67,* gene related to cell proliferation, indicating that cells under sμg have shorter cell cycle compared to cells at 1g condition (Fig. 3.2.1.3). This was validated by results from a qRT-PCR based microarray study showing significant upregulation of *cyclins B1, E1* and *D1* along with their partner CDKs (*CDK1, CDK2* and *CDK4*, respectively) under sμg compared to 1g. In addition, sμg downregulated expression of cyclin-dependent kinase inhibitor genes (INK and CIP/KIP family of inhibitors). Analysis of RNAseq data also indicated the

upregulation of multiple cell cycle related pathways in hPSC cultured on sμg conditions compared to the 1g group. All of these findings suggest that under sμg conditions hPSC have shortened cell cycle and this may be supported by the enhanced self-renewal and reduced susceptibility towards differentiation of hPSC, as reported previously (139, 141-143). We observed that the sμg effects on hPSC were restricted and reversible to the culture condition, as the proliferation rate returned to comparable levels of hPSC cultured in 1g condition, after cells were further expanded at 1g conditions. Interestingly, the effects of sμg on cell proliferation and telomerase activity were cell-type dependent as were not replicated in hFF.

Using RNA-sequencing analysis, we identified a significant number of DEGs in sμg when compared to 1g. Functional analysis of these genes and overlap of GO terms indicated that cells grown under sμg condition displayed enrichment of biological process GO terms, including mRNA processing, mRNA stability, translation, regulation of transcription, chromatin organization and telomerase maintenance, all of which align well with our results discussed above and might be responsible for the enhanced proliferation and self-renewal observed under sμg. Multiple members of the ubiquitin proteasome system were upregulated under sμg culture condition, and we verified the upregulation at RNA and protein level of PSMD11 under sμg (Fig. 3.2.2.2). This indicates that the proteolytic activity of the proteasome complex, 26S/30S proteasome is enhanced under sμg. It has been established that both m ESC and hPSC exhibit increased levels of proteasome activity and assembly of the 26S/30S proteasomes (144, 145). This upregulation has been linked to increased levels of the 19S proteasome subunit PSMD11/RPN-6 (144, 146), an essential subunit for the assembly and activity of the

26S/30S proteasome (147). It is known that in hPSC, PSMD11 maintains self-renewal by protecting the expression of pluripotency markers and by targeting the degradation of germ layer specific markers (144). In addition, it has been shown that differentiation of hPSC results in a downregulated expression of PSMD11/RPN6 with subsequently reduced proteasomal activity and a reduction in the amount of assembled proteasome complexes. The downregulated expression of PSMD11/RPN6 during differentiation is accompanied by a decrease in hydrolytic activity of the proteasome complex, suggesting that PSMD11/RPN6 is essential for preserving the activity of the proteasome. Based on this information and our results, we concluded that under sμg conditions the ubiquitin proteasome system is participating in the enhanced self-renewal of hPSC.

4.4: CD49f is a Reliable Biomarker to Identify Functional MSC

Mesenchymal stem cells (MSC) are multipotent cells that adhere to plastic, have a fibroblast-like morphology, express a specific set of surface antigens, and differentiate into adipocytes, chondrocytes, and osteocytes (148). Clinically, MSC are of interest for their ability to modulate the immune system as well as their potential to regenerate tissues. However, the translation of MSC-based therapies has been hindered by the heterogeneity of the isolated cells as well as the lack of standardized methods for their definition and characterization. At the forefront of these issues is the lack of MSC-specific reliable markers that can be used to conclusively isolate and characterize MSC. This heterogeneity can increase experimental variability, decrease the efficiency of differentiation, and contribute to conflicting data in the literature. In an attempt to increase consistency in the definition and verification of MSC, in 2006 the International Society for Cellular Therapy (ISCT) proposed minimal criteria for the definition of

human MSC based on plastic adherence, multipotency, positive expression of cells surface markers CD73, CD90 and CD105, and negative for hematopoietic and endothelial markers (such as MHC-II, CD11b, CD14, CD34, CD45, and CD31)(149). However, major laggings concerning the definition of MSC still persists, particularly, the observations that several defining biomarkers are also expressed in fibroblasts and remain expressed in MSC that can no longer differentiate (150, 151). This suggests that these biomarkers are not cell-type-specific, nor are they truly indicative of undifferentiated MSC. On this verge several other biomarkers have been proposed to identify MSC.

Recently, we and other have consistently associated the expression of CD49f in MSC with cells that show higher clonogenicity, and differentiation potential *in vitro*, which has also been correlated with early passages, and the subsequent decrease in both expression of CD49f and differentiation capacity in older passages (152-157). Besides this, we also have collected evidence that CD49f is a biomarker that have been identified in all stem cell populations and plays an important role in self-renewal of different stem cell populations, including MSC (5). All these evidences strongly indicate that functional stem cells can be identified by CD49f expression levels, and justify the need for deeper investigation in the CD49f-positive MSC subpopulation on their potential to be used for regenerative medicine, and in their transcriptome that confers their stemness, both remaining as a gap in knowledge.

My hypothesis is CD49f positive cells have reproducibly higher differentiation potentiality, and stemness, and hence, the comparative RNA profiles of CD49f positive vs CD49f negative MSC will enable the identification of fundamental transcriptome

profile differences, which is important for a clear understanding and use of MSC in biomedical applications.

As discussed before, MSC are characterized by expression of cell surface biomarkers and their ability to differentiate into bone, cartilage and fat. However, the current biomarkers used to identify these cell populations are not cell-type-specific or indicative of the differentiation status of these cells and are therefore unreliable. As we and other have shown that CD49f has been identified as a biomarker that is commonly expressed in all identified stem cell types, including MSC, and that it plays an important role in self-renewal of different stem cell populations, here, I aim to establish this transmembrane protein as a reliable biomarker that defines functional MSC, and set following hypothesis: the expression of CD49f can be used to identify a functional MSC population.

CHAPTER FIVE

CONCLUSIONS AND FUTURE DIRECTIONS

5.1: Overall Conclusions

In summary, we have established a chemically defined and xeno-free culture condition for long-term maintenance and derivation of hPSC using our optimized and standardized 10% HSt-PMEDSAH-g dishes. The karyotype of hPSC remains stable after long-term culturing *in vitro*. Furthermore, the chemically defined and xeno-free culturing system also permits efficient derivation of hiPSC from human fibroblast through reprogramming. The xeno-free and chemically defined culture conditions described in this protocol are ideal for reducing lot-to-lot variation and increasing reproducibility, which can ensure consistency for the use of hPSC in both basic research and clinical applications. The long-term maintenance of hPSC without compromising safety and functionality in this defined culture system will reduce the economic burden for large-scale expansions for various applications. Our culture system has promising potentials for the wide applications of hPSC in *in vitro* studies to better understand developmental biology, and paves the way for translating hESC and hiPSC technology to the clinic.

Based on our results and other previous reports regarding the crosstalk between stem cell and cell cycle machineries (61, 102, 137, 139, 158), we have developed a model explaining the regulation of proliferation and self-renewal of hPSC by sμg (Fig. 3.2.3). The canonical model highlights the interplay between the core set of pluripotency TF, including OCT4, SOX2, and NANOG, and a common transmembrane glycoprotein heterodimeric complex formed by ITGA6 and ITGB1, for maintaining proliferation and

self-renewal of hPSC by interacting with major regulators of the cell cycle. Under sμg condition, our model shows that hPSC enhanced their proliferation and self-renewal, by overexpression of the core set of pluripotent TFs complex and glycoprotein heterodimeric complex signaling networks (both represented in brown color). In addition, the ubiquitin proteasome system (represented by PSDM11) is also upregulated (represented in brown color), providing further support to the self-renewal machinery. In turn, the core of pluripotent TF complex may upregulate the expression of major cell cycle regulators (represented in green) maintaining shorter cell cycle, and reducing the susceptibility towards differentiation, resulting in an enhanced self-renewal of hPSC. These findings are critical to both space science and cell biology due to its potential to decipher the effect of ug on humans at a cellular level as well as in the regeneration of tissues in the human body, and to use these alterations to better understand and solve spaceflight-based problems.

In addition, our results emphasized ITGA6 **(**CD49f) as a reliable biomarker that better define the functional status of MSC (SSC). This has significant implications in regenerative medicine. As many clinical trials using stem cells defined as skeletal stem cells are ongoing currently, these cells are likely defined using standard characterization, which we show identifies functional and non-functional cells. Thus, we propose inclusion of new biomarkers such as ITGA6 (CD49f) that better identify functional SSCs to obtain consistent outcomes and success in SSC based therapies.

5.2: Future Directions

While the findings of this dissertation have been very informative, there are many experiments that still need to be performed as well as, some of which are discussed below:

5.2.1: Determine the Enhanced *In Vivo* Osteogenic Potential of CD49f^{pos} MSC in Regenerating Craniofacial Skeletal Defects

The aim of this project is to identify MSC that can better regenerate clinically relevant craniofacial defects *in vivo*. I am proposing to use the calvaria defect rat model because the critical size cranial defect provides a convenient and meaningful orthotopic site to test and quantify the osteogenic capability of CD49f^{pos} MSC in the context of a living animal. Besides, we have experience transplanting MSC derived from human iPSC into this model with successful human bone formation(159).

Our preliminary studies indicate that CD49f^{pos} MSC have enhanced stemness in relation to CD49f^{neg} MSC obtained from the same pool of parental cells. These findings are supported by recent publication (155), nevertheless, all these studies have been done in *in vitro* conditions, remaining as gap of knowledge to demonstrate the *in vivo* osteogenic potential of CD49f^{pos} MSC.

The hypothesis for this project is 'CD49f^{pos} cells enriched from both bone marrow-derived MSC and the differentiation of pluripotent stem cells have reproducibly higher potential to generate new bone, *in vivo'*.

5.2.2: Determine the Transcriptome Profile of MSC that Sustain Enhanced Stemness in CD49f^{pos} Cells

This project is designed to shed light on the network of transcription factors that will give an identity to MSC. As mentioned early, the current definition of MSC

generates heterogeneous populations that contain stem cells, progenitor cells and differentiated cells, all of them expressing the combination of biomarkers CD105, CD90, and CD73, low expression of MHC-I, and be negative for MHC-II, CD11b, CD14, CD34, CD45, and CD31. This issue is magnified by the isolation of MSC from different tissue, the method of culture and other factors that results in inconsistent populations and obscure the interpretation of data aiming to determine the transcriptome of MSC. Our(152) and other(155) previously published data, and our preliminary data shows that a subpopulation of MSC expressing CD49f is able to isolate cells with enhanced *in vitro* stemness properties, in terms of clonogenicity and differentiation (Fig. 3.3.1-3.3.3). Here, I propose to use the $CD49f^{pos}$ homogenous population to determine the transcriptome profile giving stemness to MSC. The hypothesis is, 'comparative RNA profiles of $CD49f^{pos}$ vs $CD49f^{neg}$ MSC will enable the identification of fundamental transcriptome profile differences that confer MSC stemness'.

5.3: Overall Approach to Investigate the Role of CD49f in MSC

Based on previous findings and preliminary studies I propose to establish CD49f as a reliable biomarker to identify functional MSC with enhanced stemness, and to determine the *in vivo* potential of $CD49f^{pos}$ MSC for osteogenic regeneration of clinically relevant calvaria defects and compare it to the osteogenic potential of $CD49f^{neg}$ MSC, and complete MSC populations derived from bone marrow extractions and from the differentiation of human iPSC. I also propose to determine the transcriptome that define the enhanced stemness of $CD49f^{pos}$ MSC. In Fig. 5.2.2.1**,** I outline the general approach that will be taken to obtain $CD49f^{pos}$ and $CD49f^{neg}$ MSC and Fig. 5.2.2.2 represents the preliminary date about the TF bound to $CD49f^{pos}$ MSC. The primary human bone marrow

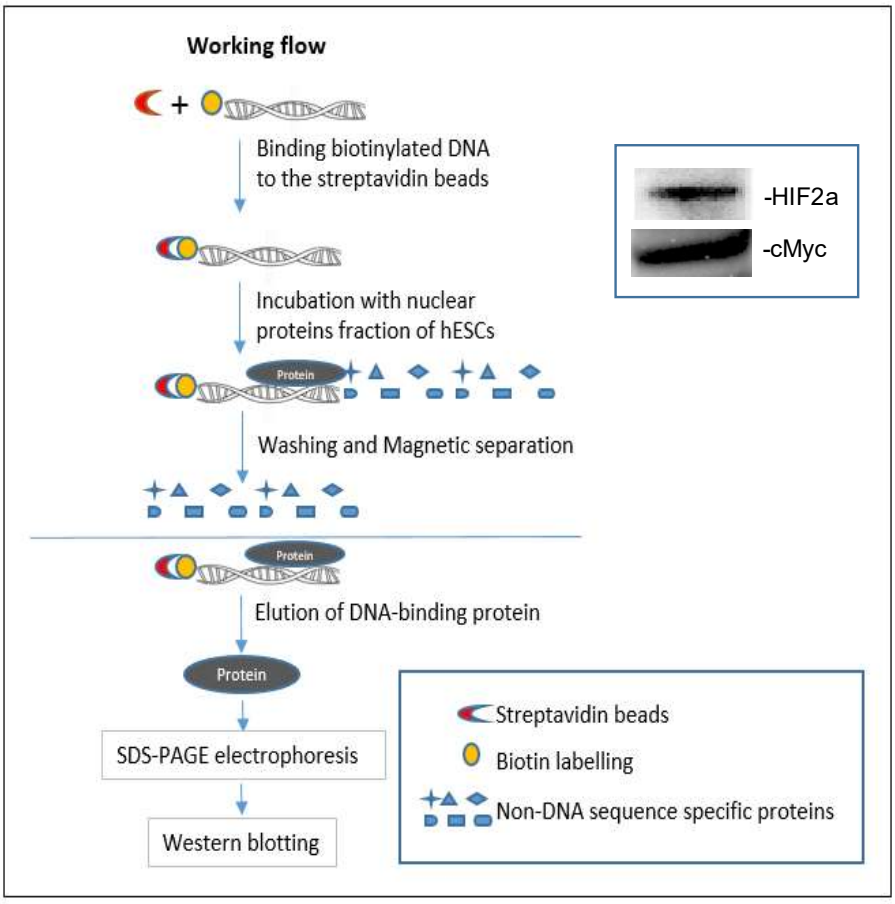

Figure 5.2.2.1: Schematic strategy to identify CD49f DNA binding-transcription factors in MSC. The illustration indicates the steps to identify transcription factors present in the CD49f^{pos} MSC with regulatory activity over *CD49f*. The inlet shows the detection of HIF2α and cMYC as CD49f DNA binding proteins in hESC.

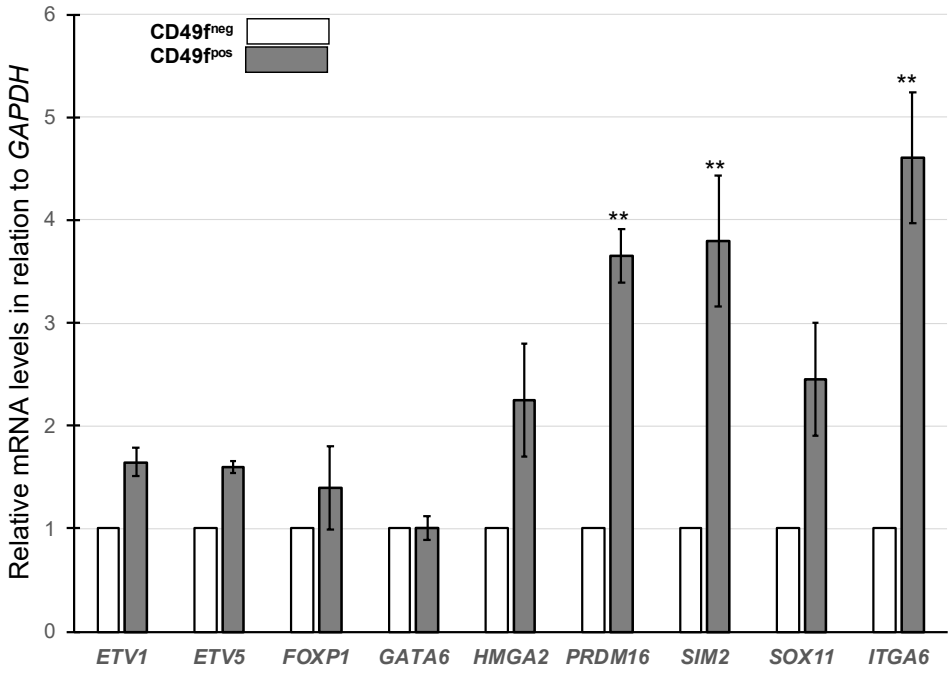

Figure 5.2.2.2: Preliminary identification of transcription factors in CD49f^{pos} MSC.

derived MSC will be obtained from cell/tissue banks, while human iPSC will be used for differentiation into MSC, using protocols routinely used in our lab (133, 152, 159). The primary MSC and the parental cells use for derivation iPSC will be from female and male origin. The MSC populations will be characterized following standard protocols(149). Cells at passage 3 will be used for all experiments. Separation of MSC into $CD49f^{pos}$ and $CD49f^{neg}$ cells will be done by fluorescent activated cell sorting using the services of the Flow Cell Sorting Core Facility of the Department of Biological Sciences at Oakland University.

Moreover, as depicted in Fig. 5.3, MSC will be obtained from primary cells of bone marrow aspirates or after the differentiation of hiPSC. After their standard characterization (Aim 1- using CD49f to identify functional MSC with enhanced stemness), MSC will be sorted into $CD49f^{pos}$ and $CD49f^{neg}$ cells, and be used for experiments described in Aims 2 and 3.

Data generated from this proposal will be fundamental to our future goals that include the reprogramming of somatic cells into functional induced (i)MSC using known transcription factors. Until know this has not been achieved because master regulators of MSC remain unknown. iMSC will represent a constant personalized cell source for use in multiple biomedical applications, including the treatment of bone defects with tissue engineering constructs.

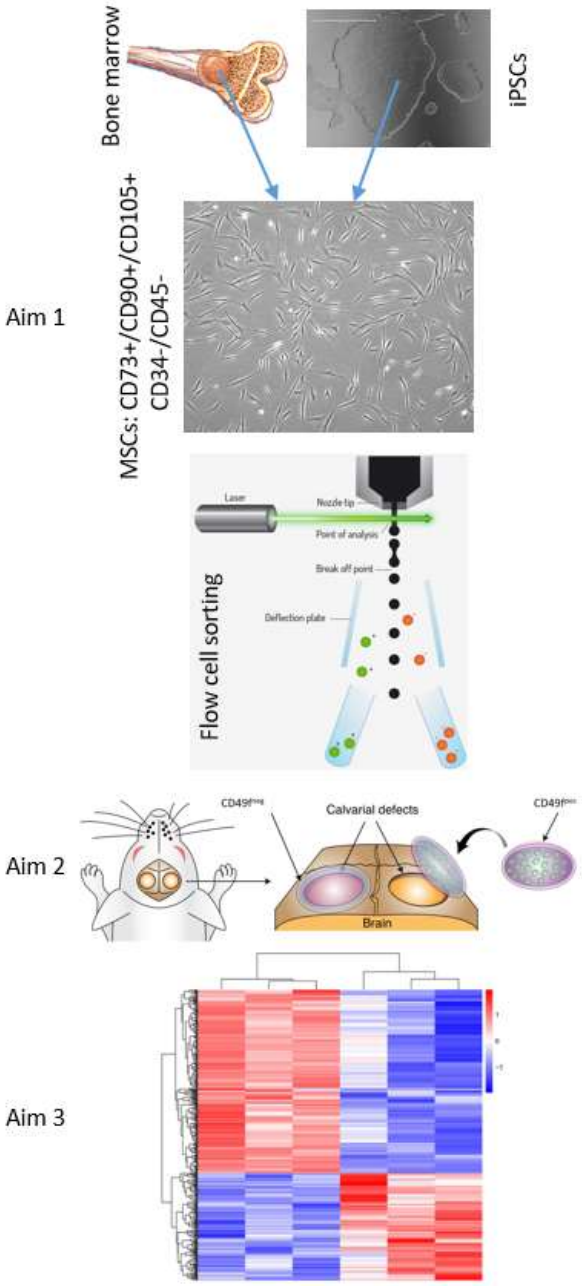

Figure 5.3: Schematic representation to determine the in vivo osteogenic potential of CD49f^{pos} MSC and their transcriptome.

References

1. Morrison SJ, Kimble J. Asymmetric and symmetric stem-cell divisions in development and cancer. Nature. 2006;441(7097):1068-74.
2. Hynes RO. Integrins: versatility, modulation, and signaling in cell adhesion. Cell. 1992;69(1):11-25.
3. Hynes RO, Naba A. Overview of the matrisome--an inventory of extracellular matrix constituents and functions. Cold Spring Harb Perspect Biol. 2012;4(1):a004903.
4. Barczyk M, Carracedo S, Gullberg D. Integrins. Cell Tissue Res. 2010;339(1):269-80.
5. Krebsbach PH, Villa-Diaz LG. The Role of Integrin alpha6 (CD49f) in Stem Cells: More than a Conserved Biomarker. Stem Cells Dev. 2017;26(15):1090-9.
6. Stingl J, Eirew P, Ricketson I, Shackleton M, Vaillant F, Choi D, et al. Purification and unique properties of mammary epithelial stem cells. Nature. 2006;439(7079):993-7.
7. Wiencierz AM, Kernbach M, Ecklebe J, Monnerat G, Tomiuk S, Raulf A, et al. Differential Expression Levels of Integrin alpha6 Enable the Selective Identification and Isolation of Atrial and Ventricular Cardiomyocytes. PLoS One. 2015;10(11):e0143538.
8. Chernaya O, Shinin V, Liu Y, Minshall RD. Behavioral heterogeneity of adult mouse lung epithelial progenitor cells. Stem Cells Dev. 2014;23(22):2744-57.

9. McQualter JL, Yuen K, Williams B, Bertoncello I. Evidence of an epithelial stem/progenitor cell hierarchy in the adult mouse lung. Proc Natl Acad Sci U S A. 2010;107(4):1414-9.

10. Shinohara T, Avarbock MR, Brinster RL. beta1- and alpha6-integrin are surface markers on mouse spermatogonial stem cells. Proc Natl Acad Sci U S A. 1999;96(10):5504-9.

11. Schober M, Fuchs E. Tumor-initiating stem cells of squamous cell carcinomas and their control by TGF-beta and integrin/focal adhesion kinase (FAK) signaling. Proc Natl Acad Sci U S A. 2011;108(26):10544-9.

12. Xu CH, Inokuma MS, Denham J, Golds K, Kundu P, Gold JD, et al. Feeder-free growth of undifferentiated human embryonic stem cells. Nature Biotechnology. 2001;19(10):971-4.

13. Notta F, Doulatov S, Laurenti E, Poeppl A, Jurisica I, Dick JE. Isolation of single human hematopoietic stem cells capable of long-term multilineage engraftment. Science. 2011;333(6039):218-21.

14. Fujikawa T, Hirose T, Fujii H, Oe S, Yasuchika K, Azuma H, et al. Purification of adult hepatic progenitor cells using green fluorescent protein (GFP)-transgenic mice and fluorescence-activated cell sorting. J Hepatol. 2003;39(2):162-70.

15. Hall PE, Lathia JD, Miller NG, Caldwell MA, ffrench-Constant C. Integrins are markers of human neural stem cells. Stem Cells. 2006;24(9):2078-84.

16. Igarashi T, Shimmura S, Yoshida S, Tonogi M, Shinozaki N, Yamane GY. Isolation of oral epithelial progenitors using collagen IV. Oral Dis. 2008;14(5):413-8.

17. Kurata R, Futaki S, Nakano I, Tanemura A, Murota H, Katayama I, et al. Isolation and characterization of sweat gland myoepithelial cells from human skin. Cell Struct Funct. 2014;39(2):101-12.

18. Osada M, Singh VJ, Wu K, Sant'Angelo DB, Pezzano M. Label retention identifies a multipotent mesenchymal stem cell-like population in the postnatal thymus. PLoS One. 2013;8(12):e83024.

19. Goel HL, Pursell B, Chang C, Shaw LM, Mao J, Simin K, et al. GLI1 regulates a novel neuropilin-2/alpha6beta1 integrin based autocrine pathway that contributes to breast cancer initiation. EMBO Mol Med. 2013;5(4):488-508.

20. Jung JG, Kim DK, Park TS, Lee SD, Lim JM, Han JY. Development of novel markers for the characterization of chicken primordial germ cells. Stem Cells. 2005;23(5):689-98.

21. Chen Z, de Paiva CS, Luo L, Kretzer FL, Pflugfelder SC, Li DQ. Characterization of putative stem cell phenotype in human limbal epithelia. Stem Cells. 2004;22(3):355-66.

22. Chang C, Goel HL, Gao H, Pursell B, Shultz LD, Greiner DL, et al. A laminin 511 matrix is regulated by TAZ and functions as the ligand for the alpha6Bbeta1 integrin to sustain breast cancer stem cells. Genes Dev. 2015;29(1):1-6.

23. Lathia JD, Gallagher J, Heddleston JM, Wang J, Eyler CE, Macswords J, et al. Integrin alpha 6 regulates glioblastoma stem cells. Cell Stem Cell. 2010;6(5):421-32.

24. Fujimoto K, Beauchamp RD, Whitehead RH. Identification and isolation of candidate human colonic clonogenic cells based on cell surface integrin expression. Gastroenterology. 2002;123(6):1941-8.

25. Morgner J, Ghatak S, Jakobi T, Dieterich C, Aumailley M, Wickstrom SA. Integrin-linked kinase regulates the niche of quiescent epidermal stem cells. Nat Commun. 2015;6:8198.

26. Shen Q, Wang Y, Kokovay E, Lin G, Chuang SM, Goderie SK, et al. Adult SVZ stem cells lie in a vascular niche: a quantitative analysis of niche cell-cell interactions. Cell Stem Cell. 2008;3(3):289-300.

27. Leivo I, Vaheri A, Timpl R, Wartiovaara J. Appearance and distribution of collagens and laminin in the early mouse embryo. Dev Biol. 1980;76(1):100-14.

28. Castaldo C, Di Meglio F, Nurzynska D, Romano G, Maiello C, Bancone C, et al. CD117-positive cells in adult human heart are localized in the subepicardium, and their activation is associated with laminin-1 and alpha6 integrin expression. Stem Cells. 2008;26(7):1723-31.

29. Brizzi MF, Tarone G, Defilippi P. Extracellular matrix, integrins, and growth factors as tailors of the stem cell niche. Curr Opin Cell Biol. 2012;24(5):645-51.

30. Abdelalim EM. Recent Advances in Stem Cells: From Basic Research to Clinical Applications. 1 ed: Humana Press; 2016.

31. El Barky AR, Ezz AAH, Alm-Eldeen AA, Hussein SA, Hafez YA, Mohamed TM. Can Stem Cells Ameliorate the Pancreatic Damage Induced by Streptozotocin in Rats? Can J Diabetes. 2018;42(1):61-70.

32. Zakrzewski W, Dobrzynski M, Szymonowicz M, Rybak Z. Stem cells: past, present, and future. Stem Cell Res Ther. 2019;10(1):68.

33. Marikawa Y, Alarcon VB. Establishment of trophectoderm and inner cell mass lineages in the mouse embryo. Mol Reprod Dev. 2009;76(11):1019-32.

34. Sukoyan MA, Vatolin SY, Golubitsa AN, Zhelezova AI, Semenova LA, Serov OL. Embryonic stem cells derived from morulae, inner cell mass, and blastocysts of mink: comparisons of their pluripotencies. Mol Reprod Dev. 1993;36(2):148-58.

35. Shahbazi MN. Mechanisms of human embryo development: from cell fate to tissue shape and back. Development. 2020;147(14).

36. Miura Y. [Basics and clinical application of human mesenchymal stromal/stem cells]. Rinsho Ketsueki. 2015;56(10):2195-204.

37. Carpenter MK, Rosler ES, Fisk GJ, Brandenberger R, Ares X, Miura T, et al. Properties of four human embryonic stem cell lines maintained in a feeder-free culture system. Dev Dyn. 2004;229(2):243-58.

38. Takahashi K, Yamanaka S. Induction of pluripotent stem cells from mouse embryonic and adult fibroblast cultures by defined factors. Cell. 2006;126(4):663-76.

39. Konstantinov IE. In search of Alexander A. Maximow: the man behind the unitarian theory of hematopoiesis. Perspect Biol Med. 2000;43(2):269-76.

40. Siminovitch L, McCulloch EA, Till JE. The Distribution of Colony-Forming Cells among Spleen Colonies. J Cell Comp Physiol. 1963;62:327-36.

41. Evans MJ, Kaufman MH. Establishment in culture of pluripotential cells from mouse embryos. Nature. 1981;292(5819):154-6.

42. Eguizabal C, Aran B, Chuva de Sousa Lopes SM, Geens M, Heindryckx B, Panula S, et al. Two decades of embryonic stem cells: a historical overview. Hum Reprod Open. 2019;2019(1):hoy024.

43. Becker AJ, Mc CE, Till JE. Cytological demonstration of the clonal nature of spleen colonies derived from transplanted mouse marrow cells. Nature. 1963;197:452-4.

44. Stem Cell Timeline. Heart Views. 2015;16(2):72-3.

45. Menasche P, Vanneaux V, Hagege A, Bel A, Cholley B, Cacciapuoti I, et al. Human embryonic stem cell-derived cardiac progenitors for severe heart failure treatment: first clinical case report. Eur Heart J. 2015;36(30):2011-7.

46. Schwartz SD, Regillo CD, Lam BL, Eliott D, Rosenfeld PJ, Gregori NZ, et al. Human embryonic stem cell-derived retinal pigment epithelium in patients with age-related macular degeneration and Stargardt's macular dystrophy: follow-up of two open-label phase 1/2 studies. Lancet. 2015;385(9967):509-16.

47. Ilic D, Ogilvie C. Concise Review: Human Embryonic Stem Cells-What Have We Done? What Are We Doing? Where Are We Going? Stem Cells. 2017;35(1):17-25.

48. Pennings S, Liu KJ, Qian H. The Stem Cell Niche: Interactions between Stem Cells and Their Environment. Stem Cells Int. 2018;2018:4879379.

49. Bigoni-Ordonez GD, Czarnowski D, Parsons T, Madlambayan GJ, Villa-Diaz LG. Integrin alpha6 (CD49f), The Microenvironment and Cancer Stem Cells. Curr Stem Cell Res Ther. 2018.

50. Guilak F, Cohen DM, Estes BT, Gimble JM, Liedtke W, Chen CS. Control of stem cell fate by physical interactions with the extracellular matrix. Cell Stem Cell. 2009;5(1):17-26.

51. Kfoury Y, Scadden DT. Mesenchymal cell contributions to the stem cell niche. Cell Stem Cell. 2015;16(3):239-53.

52. Gattazzo F, Urciuolo A, Bonaldo P. Extracellular matrix: a dynamic microenvironment for stem cell niche. Biochim Biophys Acta. 2014;1840(8):2506-19.

53. Hynes RO, Lander AD. Contact and adhesive specificities in the associations, migrations, and targeting of cells and axons. Cell. 1992;68(2):303-22.

54. McDonald JA. Extracellular matrix assembly. Methods Enzymol. 1994;245:518-31.

55. Hay ED. Extracellular matrix. J Cell Biol. 1981;91(3 Pt 2):205s-23s.

56. Tamkun JW, DeSimone DW, Fonda D, Patel RS, Buck C, Horwitz AF, et al. Structure of integrin, a glycoprotein involved in the transmembrane linkage between fibronectin and actin. Cell. 1986;46(2):271-82.

57. Hynes RO. The emergence of integrins: a personal and historical perspective. Matrix Biol. 2004;23(6):333-40.

58. Campbell ID, Humphries MJ. Integrin structure, activation, and interactions. Cold Spring Harb Perspect Biol. 2011;3(3).

59. Hynes RO. Integrins: bidirectional, allosteric signaling machines. Cell. 2002;110(6):673-87.

60. Askari JA, Tynan CJ, Webb SE, Martin-Fernandez ML, Ballestrem C, Humphries MJ. Focal adhesions are sites of integrin extension. J Cell Biol. 2010;188(6):891-903.

61. Villa-Diaz LG, Kim JK, Laperle A, Palecek SP, Krebsbach PH. Inhibition of Focal Adhesion Kinase Signaling by Integrin alpha6beta1 Supports Human Pluripotent Stem Cell Self-Renewal. Stem Cells. 2016;34(7):1753-64.

62. Chen W, Villa-Diaz LG, Sun Y, Weng S, Kim JK, Lam RH, et al. Nanotopography influences adhesion, spreading, and self-renewal of human embryonic stem cells. ACS Nano. 2012;6(5):4094-103.

63. Humphries MJ, Symonds EJ, Mould AP. Mapping functional residues onto integrin crystal structures. Curr Opin Struct Biol. 2003;13(2):236-43.

64. Lee JO, Rieu P, Arnaout MA, Liddington R. Crystal structure of the A domain from the alpha subunit of integrin CR3 (CD11b/CD18). Cell. 1995;80(4):631-8.

65. Xiao T, Takagi J, Coller BS, Wang JH, Springer TA. Structural basis for allostery in integrins and binding to fibrinogen-mimetic therapeutics. Nature. 2004;432(7013):59-67.

66. Ben-David U, Cowell IG, Austin CA, Benvenisty N. Brief reports: Controlling the survival of human pluripotent stem cells by small molecule-based targeting of topoisomerase II alpha. Stem Cells. 2015;33(3):1013-9.

67. Harburger DS, Calderwood DA. Integrin signalling at a glance. J Cell Sci. 2009;122(Pt 2):159-63.

68. Zaidel-Bar R, Itzkovitz S, Ma'ayan A, Iyengar R, Geiger B. Functional atlas of the integrin adhesome. Nat Cell Biol. 2007;9(8):858-67.

69. Liu S, Calderwood DA, Ginsberg MH. Integrin cytoplasmic domain-binding proteins. J Cell Sci. 2000;113 (Pt 20):3563-71.

70. He S, Nakada D, Morrison SJ. Mechanisms of stem cell self-renewal. Annu Rev Cell Dev Biol. 2009;25:377-406.

71. Shahriyari L, Komarova NL. Symmetric vs. asymmetric stem cell divisions: an adaptation against cancer? PLoS One. 2013;8(10):e76195.

72. Orford KW, Scadden DT. Deconstructing stem cell self-renewal: genetic insights into cell-cycle regulation. Nat Rev Genet. 2008;9(2):115-28.

73. Vitillo L, Kimber SJ. Integrin and FAK Regulation of Human Pluripotent Stem Cells. Curr Stem Cell Rep. 2017;3(4):358-65.

74. Wong RC, Tellis I, Jamshidi P, Pera M, Pebay A. Anti-apoptotic effect of sphingosine-1-phosphate and platelet-derived growth factor in human embryonic stem cells. Stem Cells Dev. 2007;16(6):989-1001.

75. Teramura T, Takehara T, Onodera Y, Nakagawa K, Hamanishi C, Fukuda K. Mechanical stimulation of cyclic tensile strain induces reduction of pluripotent related gene expressions via activation of Rho/ROCK and subsequent decreasing of AKT phosphorylation in human induced pluripotent stem cells. Biochem Biophys Res Commun. 2012;417(2):836-41.

76. Kinehara M, Kawamura S, Tateyama D, Suga M, Matsumura H, Mimura S, et al. Protein kinase C regulates human pluripotent stem cell self-renewal. PLoS One. 2013;8(1):e54122.

77. Qian H, Tryggvason K, Jacobsen SE, Ekblom M. Contribution of alpha6 integrins to hematopoietic stem and progenitor cell homing to bone marrow and collaboration with alpha4 integrins. Blood. 2006;107(9):3503-10.

78. Watt FM. Role of integrins in regulating epidermal adhesion, growth and differentiation. EMBO J. 2002;21(15):3919-26.

79. Akhtar N, Streuli CH. An integrin-ILK-microtubule network orients cell polarity and lumen formation in glandular epithelium. Nat Cell Biol. 2013;15(1):17-27.

80. Domogatskaya A, Rodin S, Boutaud A, Tryggvason K. Laminin-511 but not -332, -111, or -411 enables mouse embryonic stem cell self-renewal in vitro. Stem Cells. 2008;26(11):2800-9.

81. Gu YC, Kortesmaa J, Tryggvason K, Persson J, Ekblom P, Jacobsen SE, et al. Laminin isoform-specific promotion of adhesion and migration of human bone marrow progenitor cells. Blood. 2003;101(3):877-85.

82. Sun Y, Villa-Diaz LG, Lam RH, Chen W, Krebsbach PH, Fu J. Mechanics regulates fate decisions of human embryonic stem cells. PLoS One. 2012;7(5):e37178.

83. Eiermann P, Kopp S, Hauslage J, Hemmersbach R, Gerzer R, Ivanova K. Adaptation of a 2-D Clinostat for Simulated Microgravity Experiments with Adherent Cells. Microgravity Science and Technology. 2013;25(3):153-9.

84. Watanabe K, Ueno M, Kamiya D, Nishiyama A, Matsumura M, Wataya T, et al. A ROCK inhibitor permits survival of dissociated human embryonic stem cells. Nat Biotechnol. 2007;25(6):681-6.

85. Yao S, Chen S, Clark J, Hao E, Beattie GM, Hayek A, et al. Long-term self-renewal and directed differentiation of human embryonic stem cells in chemically defined conditions. Proc Natl Acad Sci U S A. 2006;103(18):6907-12.

86. Livak KJ, Schmittgen TD. Analysis of relative gene expression data using real-time quantitative PCR and the 2(-Delta Delta C(T)) Method. Methods. 2001;25(4):402-8.

87. Dallabrida SM, Ismail N, Oberle JR, Himes BE, Rupnick MA. Angiopoietin-1 promotes cardiac and skeletal myocyte survival through integrins. Circ Res. 2005;96(4):e8-24.

88. Carlson TR, Feng Y, Maisonpierre PC, Mrksich M, Morla AO. Direct cell adhesion to the angiopoietins mediated by integrins. J Biol Chem. 2001;276(28):26516-25.

89. Merten OW. Advances in cell culture: anchorage dependence. Philos Trans R Soc Lond B Biol Sci. 2015;370(1661):20140040.

90. Prowse ABJ, Chong F, Gray PP, Munro TP. Stem cell integrins: Implications for ex-vivo culture and cellular therapies. Stem Cell Research. 2011;6(1):1-12.

91. Paradise RK, Lauffenburger DA, Van Vliet KJ. Acidic extracellular pH promotes activation of integrin α(v)β(3). PLoS One. 2011;6(1):e15746.

92. Margolis LB, Rozovskaja IA, Cragoe E. Intracellular pH and cell adhesion to solid substrate. FEBS Lett. 1988;234(2):449-50.

93. Searles GE, Dixon WT, Thomas PD, Jimbow K. Divalent cations control cell-substrat adhesion and laminin expression in normal and malignant human melanocytes in early and late stages of cellular differentiation. J Invest Dermatol. 1995;105(2):301-8.

94. Attramadal A. The effect of divalent cations on cell adhesion. J Periodontal Res. 1969;4(4):281-5.

95. Attramadal A. The effect of divalent cations on cell adhesion in vitro. J Periodontal Res. 1969;4(2):166.

96. Lévesque JP, Haylock DN, Simmons PJ. Cytokine regulation of proliferation and cell adhesion are correlated events in human CD34+ hemopoietic progenitors. Blood. 1996;88(4):1168-76.

97. De Angelis MT, Parrotta EI, Santamaria G, Cuda G. Short-term retinoic acid treatment sustains pluripotency and suppresses differentiation of human induced pluripotent stem cells. Cell Death Dis. 2018;9(1):6.

98. van der Valk J, Brunner D, De Smet K, Fex Svenningsen A, Honegger P, Knudsen LE, et al. Optimization of chemically defined cell culture media--replacing fetal bovine serum in mammalian in vitro methods. Toxicol In Vitro. 2010;24(4):1053-63.

99. Song Y, Yun S, Yang HJ, Yoon AY, Kim H. Aggregation of Human Eyelid Adipose-derived Stem Cells by Human Body Fluids. Dev Reprod. 2012;16(4):339-51.

100. Yang H, Lim YH, Yun S, Yoon AY, Kim H. A role of cell adhesion molecules and gelatinases in human serum-induced aggregation of human eyelid-derived stem cells in vitro. Dev Reprod. 2013;17(4):409-20.

101. O'Connor MD, Kardel MD, Iosfina I, Youssef D, Lu M, Li MM, et al. Alkaline phosphatase-positive colony formation is a sensitive, specific, and quantitative indicator of undifferentiated human embryonic stem cells. Stem Cells. 2008;26(5):1109-16.

102. Boyer LA, Lee TI, Cole MF, Johnstone SE, Levine SS, Zucker JP, et al. Core transcriptional regulatory circuitry in human embryonic stem cells. Cell. 2005;122(6):947-56.

103. Niwa H, Miyazaki J, Smith AG. Quantitative expression of Oct-3/4 defines differentiation, dedifferentiation or self-renewal of ES cells. Nat Genet. 2000;24(4):372-6.

104. Niwa H. How is pluripotency determined and maintained? Development. 2007;134(4):635-46.

105. Armstrong L, Saretzki G, Peters H, Wappler I, Evans J, Hole N, et al. Overexpression of telomerase confers growth advantage, stress resistance, and enhanced differentiation of ESCs toward the hematopoietic lineage. Stem Cells. 2005;23(4):516-29.

106. Xu RH, Chen X, Li DS, Li R, Addicks GC, Glennon C, et al. BMP4 initiates human embryonic stem cell differentiation to trophoblast. Nat Biotechnol. 2002;20(12):1261-4.

107. Maden M. Retinoic acid in the development, regeneration and maintenance of the nervous system. Nature Reviews Neuroscience. 2007;8(10):755-65.

108. Villa-Diaz LG, Ross AM, Lahann J, Krebsbach PH. Concise Review: The Evolution of human pluripotent stem cell culture: From feeder cells to synthetic coatings. Stem Cells. 2013;31(1):1-7.

109. Chen KG, Mallon BS, McKay RD, Robey PG. Human pluripotent stem cell culture: considerations for maintenance, expansion, and therapeutics. Cell Stem Cell. 2014;14(1):13-26.

110. Villa-Diaz LG, Nandivada H, Ding J, Nogueira-de-Souza NC, Krebsbach PH, O'Shea KS, et al. Synthetic polymer coatings for long-term growth of human embryonic stem cells. Nat Biotechnol. 2010;28(6):581-3.

111. Sun Y, Yong KM, Villa-Diaz LG, Zhang X, Chen W, Philson R, et al. Hippo/YAP-mediated rigidity-dependent motor neuron differentiation of human pluripotent stem cells. Nat Mater. 2014;13(6):599-604.

112. Ullrich O, Huber K, Lang K. Signal transduction in cells of the immune system in microgravity. Cell Commun Signal. 2008;6:9.

113. Sibonga JD, Spector ER, Johnston SL, Tarver WJ. Evaluating Bone Loss in ISS Astronauts. Aerosp Med Hum Perform. 2015;86(12 Suppl):A38-A44.

114. Delp MD, Charvat JM, Limoli CL, Globus RK, Ghosh P. Apollo Lunar Astronauts Show Higher Cardiovascular Disease Mortality: Possible Deep Space Radiation Effects on the Vascular Endothelium. Sci Rep. 2016;6:29901.

115. Blaber EA, Finkelstein H, Dvorochkin N, Sato KY, Yousuf R, Burns BP, et al. Microgravity Reduces the Differentiation and Regenerative Potential of Embryonic Stem Cells. Stem Cells Dev. 2015;24(22):2605-21.

116. Chen Z, Luo Q, Yuan L, Song G. Microgravity directs stem cell differentiation. Histol Histopathol. 2017;32(2):99-106.

117. Ratushnyy AY, Buravkova LB. Expression of focal adhesion genes in mesenchymal stem cells under simulated microgravity. Dokl Biochem Biophys. 2017;477(1):354-6.

118. Fuentes TI, Appleby N, Raya M, Bailey L, Hasaniya N, Stodieck L, et al. Simulated Microgravity Exerts an Age-Dependent Effect on the Differentiation of Cardiovascular Progenitors Isolated from the Human Heart. PLoS One. 2015;10(7):e0132378.

119. Chen G, Gulbranson DR, Hou Z, Bolin JM, Ruotti V, Probasco MD, et al. Chemically defined conditions for human iPSC derivation and culture. Nat Methods. 2011;8(5):424-9.

120. Xu C, Inokuma MS, Denham J, Golds K, Kundu P, Gold JD, et al. Feeder-free growth of undifferentiated human embryonic stem cells. Nat Biotechnol. 2001;19(10):971-4.

121. Rowland TJ, Miller LM, Blaschke AJ, Doss EL, Bonham AJ, Hikita ST, et al. Roles of Integrins in Human Induced Pluripotent Stem Cell Growth on Matrigel and Vitronectin. Stem Cells and Development. 2010;19(8):1231-40.

122. Meng Y, Eshghi S, Li YJ, Schmidt R, Schaffer DV, Healy KE. Characterization of integrin engagement during defined human embryonic stem cell culture. FASEB J. 2010;24(4):1056-65.

123. Jin S, Yao H, Weber JL, Melkoumian ZK, Ye K. A synthetic, xeno-free peptide surface for expansion and directed differentiation of human induced pluripotent stem cells. PLoS One. 2012;7(11):e50880.

124. Vitillo L, Baxter M, Iskender B, Whiting P, Kimber SJ. Integrin-Associated Focal Adhesion Kinase Protects Human Embryonic Stem Cells from Apoptosis, Detachment, and Differentiation. Stem Cell Reports. 2016;7(2):167-76.

125. Brindle NP, Saharinen P, Alitalo K. Signaling and functions of angiopoietin-1 in vascular protection. Circ Res. 2006;98(8):1014-23.

126. Shattil SJ, Kim C, Ginsberg MH. The final steps of integrin activation: the end game. Nat Rev Mol Cell Biol. 2010;11(4):288-300.

127. Schwartz MA, Lechene C. Adhesion is required for protein kinase C-dependent activation of the Na+/H+ antiporter by platelet-derived growth factor. Proc Natl Acad Sci U S A. 1992;89(13):6138-41.

128. Lemieux C, Maliba R, Favier J, Théorêt JF, Merhi Y, Sirois MG. Angiopoietins can directly activate endothelial cells and neutrophils to promote proinflammatory responses. Blood. 2005;105(4):1523-30.

129. Shimizu Y, Mobley JL. Distinct divalent cation requirements for integrin-mediated CD4+ T lymphocyte adhesion to ICAM-1, fibronectin, VCAM-1, and invasin. J Immunol. 1993;151(8):4106-15.

130. Zhang K, Chen J. The regulation of integrin function by divalent cations. Cell Adh Migr. 2012;6(1):20-9.

131. Haque N, Kasim NH, Rahman MT. Optimization of pre-transplantation conditions to enhance the efficacy of mesenchymal stem cells. Int J Biol Sci. 2015;11(3):324-34.

132. Takahashi K, Yamanaka S. Induced pluripotent stem cells in medicine and biology. Development. 2013;140(12):2457-61.

133. Villa-Diaz LG, Kim JK, Lahann J, Krebsbach PH. Derivation and long-term culture of transgene-free human induced pluripotent stem cells on synthetic substrates. Stem Cells Transl Med. 2014;3(12):1410-7.

134. Wang Y, An L, Jiang Y, Hang H. Effects of simulated microgravity on embryonic stem cells. PLoS One. 2011;6(12):e29214.

135. Kawahara Y, Manabe T, Matsumoto M, Kajiume T, Yuge L. LIF-free embryonic stem cell culture in simulated microgravity. PLoS One. 2009;4(7):e6343.

136. Sharova LV, Sharov AA, Piao Y, Stagg CA, Amano T, Qian Y, et al. Emergence of undifferentiated colonies from mouse embryonic stem cells undergoing differentiation by retinoic acid treatment. In Vitro Cell Dev Biol Anim. 2016;52(5):616-24.

137. Kareta MS, Sage J, Wernig M. Crosstalk between stem cell and cell cycle machineries. Curr Opin Cell Biol. 2015;37:68-74.

138. Coronado D, Godet M, Bourillot PY, Tapponnier Y, Bernat A, Petit M, et al. A short G1 phase is an intrinsic determinant of naive embryonic stem cell pluripotency. Stem Cell Research. 2013;10(1):118-31.

139. Li VC, Kirschner MW. Molecular ties between the cell cycle and differentiation in embryonic stem cells. Proc Natl Acad Sci U S A. 2014;111(26):9503-8.

140. Ghule PN, Medina R, Lengner CJ, Mandeville M, Qiao M, Dominski Z, et al. Reprogramming the pluripotent cell cycle: restoration of an abbreviated G1 phase in human induced pluripotent stem (iPS) cells. J Cell Physiol. 2011;226(5):1149-56.

141. Becker KA, Ghule PN, Therrien JA, Lian JB, Stein JL, van Wijnen AJ, et al. Self-renewal of human embryonic stem cells is supported by a shortened G1 cell cycle phase. J Cell Physiol. 2006;209(3):883-93.

142. Barta T, Dolezalova D, Holubcova Z, Hampl A. Cell cycle regulation in human embryonic stem cells: links to adaptation to cell culture. Exp Biol Med (Maywood). 2013;238(3):271-5.

143. Kapinas K, Grandy R, Ghule P, Medina R, Becker K, Pardee A, et al. The abbreviated pluripotent cell cycle. J Cell Physiol. 2013;228(1):9-20.

144. Vilchez D, Boyer L, Morantte I, Lutz M, Merkwirth C, Joyce D, et al. Increased proteasome activity in human embryonic stem cells is regulated by PSMD11. Nature. 2012;489(7415):304-8.

145. Buckley SM, Aranda-Orgilles B, Strikoudis A, Apostolou E, Loizou E, Moran-Crusio K, et al. Regulation of pluripotency and cellular reprogramming by the ubiquitin-proteasome system. Cell Stem Cell. 2012;11(6):783-98.

146. Vilchez D, Boyer L, Lutz M, Merkwirth C, Morantte I, Tse C, et al. FOXO4 is necessary for neural differentiation of human embryonic stem cells. Aging Cell. 2013;12(3):518-22.

147. Pathare GR, Nagy I, Bohn S, Unverdorben P, Hubert A, Korner R, et al. The proteasomal subunit Rpn6 is a molecular clamp holding the core and regulatory subcomplexes together. Proceedings of the National Academy of Sciences of the United States of America. 2012;109(1):149-54.

148. Friedenstein AJ. Osteogenic stem cells in bone marrow. . Heersche J.N.M. K, J.A., editor: Elsevier; 1990. 243-72 p.

149. Dominici M, Le Blanc K, Mueller I, Slaper-Cortenbach I, Marini F, Krause D, et al. Minimal criteria for defining multipotent mesenchymal stromal cells. The International Society for Cellular Therapy position statement. Cytotherapy. 2006;8(4):315-7.

150. Squillaro T, Peluso G, Galderisi U. Clinical Trials With Mesenchymal Stem Cells: An Update. Cell Transplant. 2016;25(5):829-48.

151. Bianco P, Robey PG, Simmons PJ. Mesenchymal stem cells: revisiting history, concepts, and assays. Cell Stem Cell. 2008;2(4):313-9.

152. Qiryaqoz Z, Timilsina, S., Czarnowki, D., Krebsbach, P.H., Villa-Diaz, L.G. Identification of biomarkers indicative of functional skeletal stem cells. Orthod Craniofac Res. 2019.

153. Lee RH, Seo MJ, Pulin AA, Gregory CA, Ylostalo J, Prockop DJ. The CD34-like protein PODXL and alpha6-integrin (CD49f) identify early progenitor MSCs with increased clonogenicity and migration to infarcted heart in mice. Blood. 2009;113(4):816-26.

154. Lee MW, Kim DS, Yoo KH, Kim HR, Jang IK, Lee JH, et al. Human bone marrow-derived mesenchymal stem cell gene expression patterns vary with culture conditions. Blood Res. 2013;48(2):107-14.

155. Nieto-Nicolau N, de la Torre RM, Farinas O, Savio A, Vilarrodona A, Casaroli-Marano RP. Extrinsic modulation of integrin alpha6 and progenitor cell behavior in mesenchymal stem cells. Stem Cell Res. 2020;47:101899.

156. Yang Z, Dong P, Fu X, Li Q, Ma S, Wu D, et al. CD49f Acts as an Inflammation Sensor to Regulate Differentiation, Adhesion, and Migration of Human Mesenchymal Stem Cells. Stem Cells. 2015;33(9):2798-810.

157. Yu KR, Yang SR, Jung JW, Kim H, Ko K, Han DW, et al. CD49f enhances multipotency and maintains stemness through the direct regulation of OCT4 and SOX2. Stem Cells. 2012;30(5):876-87.

158. Liu L, Michowski W, Kolodziejczyk A, Sicinski P. The cell cycle in stem cell proliferation, pluripotency and differentiation. Nat Cell Biol. 2019;21(9):1060-7.

159. Villa-Diaz LG, Brown SE, Liu Y, Ross AM, Lahann J, Parent JM, et al. Derivation of mesenchymal stem cells from human induced pluripotent stem cells cultured on synthetic substrates. Stem Cells. 2012;30(6):1174-81.